jntes

JOURNAL OF NEW TECHNOLOGIES IN ENVIRONMENTAL SCIENCE

1

2021

No. 1 Vol. 5 ISSN 2544-7017 www.jntes.tu.kielce.pl Kielce University of Technology

CONTENTS

www.jntes.tu.kielce.pl
jntes@tu.kielce.pl

The quarterly printed issues of Journal of New Technologies in Environmental Science are their original versions. The Journal published by the Kielce University of Technology.

ISSN 2544-7017

Doi: 10.53412

Alina V. KONYK
Volodymyr V. DEMCHENKO
Institute of Technical Thermophysics of the NAS of Ukraine
Corresponding author: vladimirdemcenko71@gmail.com

DOI: 10.53412/jntes-2021-1.1

INTEGRATION OF HEAT STORAGE TECHNOLOGIES IN CENTRAL HEATING SYSTEMS

Abstract: *The global energy sector is undergoing a major transformation, from increasingly greater electrification to increased use of renewable energy sources. Along with this, the areas of relevance are considered to be the directions of creating a system of district heating and cooling system of the 4th generation.*

Keywords: *district heating systems heat supply systems, heat accumulator.*

Introduction

Total saving of energy contributes to increase of efficiency of heat supply, it is realized mainly by means of network of pipelines. District heating (DHS) and cooling networks are branched pipeline transport infrastructure, used for transportation of heat energy from energy source (e.g. boilers) to numerous users. The main consumers remain apartment buildings, the private sector and industrial enterprises. In the European Union, the residential sector uses about 26.1% of final energy consumption [1]. In Ukraine, 1.6 times more initial energy is used for heat production than for electricity production. Electricity production accounts for 39%, while high-potential (T > 100°C) heat production consumes 21% and low-potential (T < 100°C) 40%, respectively. Therefore, improving the efficiency of the DH system can contribute to overall energy savings.

The main advantages of the DHS system include:

- the ability to provide heat to a significant number of customers at the same time, located over large areas;
- use of different local fuels and energy sources which makes it possible to reduce the cost of heat;
- possibility of centralized regulation of heat carrier temperature, allows to minimize heat loss;
- the system is controlled remotely by specialized organizations, provides high reliability, environmental friendliness and ease of use.

However, such a system has a number of disadvantages:

- large losses during transportation and distribution of heat;
- lack of quantitative regulation capability;
- violation of the temperature regime at peak loads.

The current state of heating networks does not meet the technical requirements. In the EU about 11% of heating systems are inefficient [2]. In Ukraine this figure reaches 17%. Thus, the ageing and breakdown of heat networks is growing and in some regions Ukraine it is to 22.3%.

Systems of accumulation and storage of thermal energy (TES) can solve the problems of unstable DHS system operation in the peak period of heat consumption, provide stable operation of boiler equipment with the highest possible efficiency, reduce the consumption of electricity and fossil fuels, as well as

significantly reduce harmful emissions into the environment. In addition, the use of TES allows to attract to the multifuel balance of renewable energy systems and secondary energy resources.

These tasks are especially relevant in the current socio-economic conditions to ensure energy security and flexibility of DHS systems, decarbonization of generation, reducing the cost of transportation and distribution of thermal energy and the prospects for transition to new advanced technologies of the fourth generation. DHS systems of the fourth generation is a modern trend of heat supply, is actively implemented in the EU, the U.S. and China. In particular, their introduction allows to solve ecological problems, so the European Union announced the "green agreement" aimed at reducing greenhouse gas emissions by 50% by 2030 compared to 1990 [3].

Purpose and objectives of the work

The purpose of this study is to investigate and justify the integration of heat storage technologies in central heating systems.

Research objectives:

- to determine the main directions of development of central heating;
- to present modern classification of heat storage technologies;
- to define perspective variants of application of technologies of heat storage in central heating systems.

Directions for development of district heating

Directions of modernization of central heating system are conditioned by mismatch of priorities of district heating enterprises and consumers. Our analysis shows that they coincide only at the level of installation of heat regulation systems and reduction of heat losses for technological needs. Consumers are interested in reducing payments for heat consumption, with maximum comfort in the premises, while suppliers of thermal energy are interested only in the transition to the multi-purpose balance and reducing the cost of heat production.

In order to increase the efficiency of using district heating, there is a tendency to lower operating temperatures in heating networks. Lower network temperatures reduce heat losses and allow the integration of low-grade waste heat and renewable energy sources.

In the future the need for heating is expected to decrease, the need for cooling in buildings will increase significantly in the coming decades. The task of an emission-free supply of heating and cooling energy is a challenge, especially in urban areas. Thus, the supply of energy by decentralized sources of supply is not acceptable. On the other hand, district heating and cooling DHS is becoming increasingly important. The development of district heating and energy storage systems are shown in Figure 1.

There is a general tendency of correspondence of stages of development of heating networks to stages of development of industries. DHS of the 1st generation emerged in the first half of the last century. This system is characterized by separate production of heat and electric energy and use of fossil fuels (coal, peat) and oil products (oil, mazut, diesel). Generation 1 DHS is characterized by high temperature of the heat carrier above 150°C and low efficiency of 50%.

Generation 2 DHS heating and hot water supply determines a mass use of natural and liquefied gas, the use of secondary energy resources (SER) in the fuel mix, compatible generation of heat and electricity, the heat carrier temperature is 115/70°C and the system efficiency is around 60%. It should be noted that thermal accumulators (TES) appear at sources of heat generation. DHS of the 2nd generation developed from the 40s to the 90s of the last century.

Generation 3 DHS unfolded in Western Europe and the U.S. from the early 2000s to 2020. They are characterized by compatible generation of heat and electricity and the use of renewable energy sources (wind, solar, geothermal heat), alternative and biological fuels and abandoning the use of fossil fossil fuels. The operating temperature of the heat carrier is 90/70°C and the efficiency of the

system has increased to 70%. Widespread use of renewable sources led to the wide introduction of heat storage technologies. It should be noted that Ukraine is currently actively developing DHS 3rd generation. Now the vast majority of energy comes from non-renewable sources such as oil, coal, natural gas and uranium, causing greenhouse gas emissions, global warming and related climate change. Counteracting these adverse phenomena is a huge challenge for modern science and economy, which calls for research on the possibility of using renewable energy sources as alternatives with solar energy and methods of production, conversion and storage being the highest. High potential for the use of heat derived from solar energy, due to the high efficiency of storage and conversion of this energy. The main elements used in this area are solar collectors and heat storage systems.

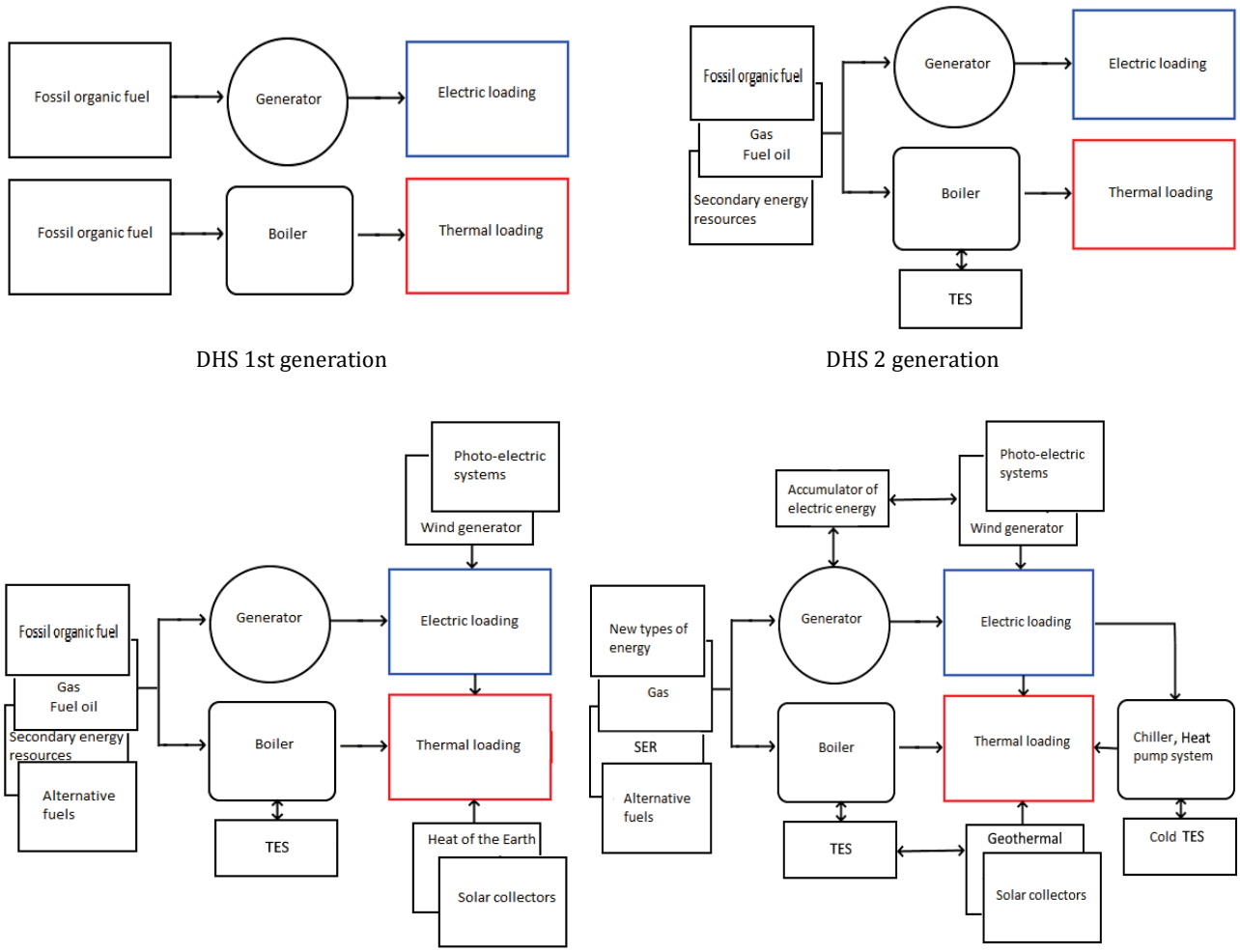

FIGURE 1. *Development of district heating and energy storage systems*

This has led to the transition to 4th generation DHS systems. The EU is currently implementing an ambitious plan to create a new generation heating, hot water and cooling system by 2050. It covers the development and introduction of new energy sources, and almost complete abandonment of the use of fossil fuels. The temperature schedule of such a system is 70°C/50°C, and the overall efficiency is envisaged above 70%. The focus is on thermal and electrical energy storage and storage systems. Scientific research carried out over many years has been aimed at developing appropriate accumulators, which will allow energy storage and will be characterized by high efficiency.

Among the various methods of heat storage are direct heat storage, latent heat storage and thermochemical energy storage. The efficiency of TES depends on the properties of the selected heat storage materials, on the conditions in which these devices are used, and on the purpose for which they are used.

Classification of technologies of storage of heat

TES technologies provide the ability to store heat or cold and use excess thermal energy for hours, days or even months. Global trends in efficiency, energy savings and security of energy systems are based on the principle of energy storage. Depending on the form of energy storage, general heat storage technologies fall into the following categories:

1. Technologies for transforming mechanical energy into thermal energy, such as hydroelectric power plants, steam turbines, Stirling engine, widespread, but characterized by low efficiency, about 30%. It should be remembered that there are thermodynamic limitations of power generation at temperatures below 340°C. Therefore, they are not used in DHS systems.
2. A large amount of heat is available between 40°C and 200°C, but there are inherent difficulties in its utilization and utilization that require separate and in-depth research. Because lowtemperature heat involves a smaller temperature gradient between the two fluid streams, large heat transfer surfaces are required for heat transfer. This limits the economic viability of their use as they require the use of a heat pump to increase the temperature of the heat transfer fluid. TES based on singlephase capacitive storage for seasonal or shortterm thermal energy storage allow the use of heat or cold from natural sources and secondary energy resources. Thermal accumulation is carried out by solid or liquid substances due to the heat capacity of the material. The capacity of heat storage in such accumulators ranges from a hundred kilowatts to hundreds of megawatts. Payback period of 4 to 6 years.
3. Hidden heat including a significant part of the energy. Thermal energy storage in the so-called latent TES systems are based on the use of materials with phase transition of organic (high molecular weight paraffins, waxes and glycols) or inorganic origin (crystalline hydrates, salt hydrates and eutectic water-salt solutions), which are characterized by high latent heat capacity. The limited use of thermal storage with phase transition can be explained by the low thermal conductivity coefficient and excessive corrosiveness of inorganic materials, as well as the change in volume during melting of materials of organic origin. Payback period of about 3 years.
4. Of general interest are technologies of use of latent chemical energy, based on adsorption processes. These are equipment for heat receiving from gas for low and medium temperatures. Zeolites and silica gel are used as the working body, air is used as the coolant. Thermal energy storage can be daily, weekly, monthly or even seasonal, depending on the volume of the working body. Payback period up to 7 years.
5. Heat accumulators based on photochemical and thermochemical reactions, thermoelectric and triboelectric principles of action have not found wide application and are currently at the stage of research trials. However, new technologies are being developed that can produce electricity directly from heat, such as thermoelectric and piezoelectric generation with subsequent storage and application for heat carrier heating.

Application of technologies storage heat is in the systems of the central heating

Centralized heating and hot water supply has a great potential for the use of main pipelines as heat accumulators, allowed by the current regulatory documents [4]. If in Western Europe DHS occupies about 10% of the total heating market, in Ukraine it reaches 70% [5]. Our research shows that the use of heat supply networks as heat storage and optimization of DHS system can reduce the total cost of primary energy up to 5%.

In addition, promising technologies of heat storage in central heating systems include heat pumps – a cost-effective technology that uses electricity to obtain heat from the ground or air for heating systems of industrial, commercial and residential buildings. However, investing in electric heat pumps is not attractive due to a lack of legislative subsidies. Large capacity heat pumps for DHS are seen as an economic and energy efficient solution [6].

Widespread stationary heat storage have been used in DHS since the first generations of heating systems. Stationary TES are used both in homes and in combination with thermal power plants, boilers and heat pumps in DHS. Moreover, TES gives the possibility to optimally control the load of boilers, reducing the consumption of fuel and energy resources and harmful emissions into the environment. Mobile thermal accumulators (M-TES) can be successfully used to combine several sources of thermal energy, combined into a single system. This is of particular importance, given the increasing use of renewable and secondary energy sources [7].

Principal technological scheme of integration of heat storage into heat supply system is shown in Figure 2 covers – direct TES on the energy source, TES on the heat network, TES of distribution heating system and M-TES on a truck.

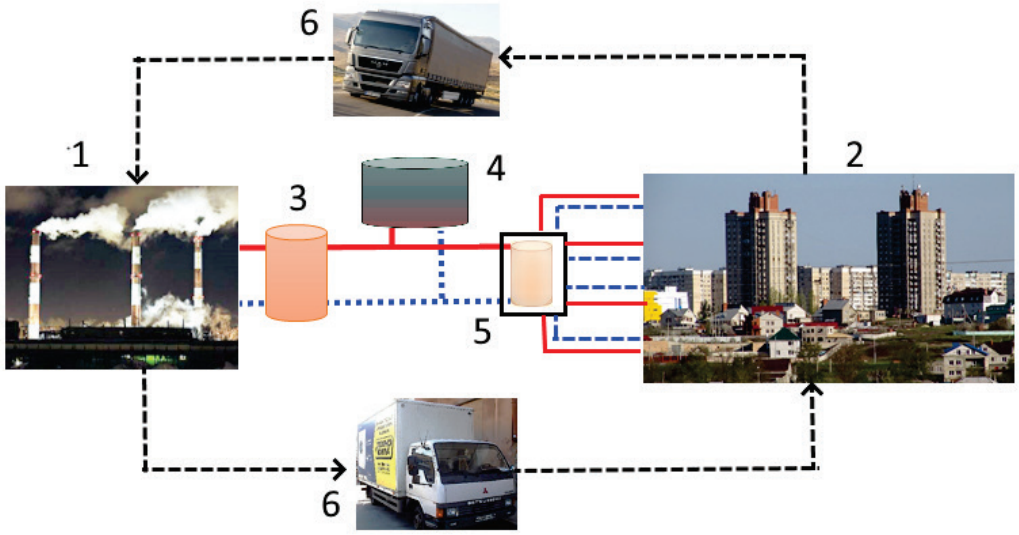

Figure 2. *Of principle flowsheet of integration of thermal storage in the DHS system, where: 1 – TES an energy source, 2 – TES is an user, 3 – TES of direct action, 4 – TES a transport network, 5 – TES of the indirect operating on distributive a network, 6 – M-TES*

The issues of improving the efficiency of district heating have a number of controversies. The first is the type of heating system of the consumer or with direct connection to the pipeline, or through a heat exchanger. The second is heat losses associated with the connection points of customers and their distance from the boiler house. The third is in the heat extraction of different customers, which may have different energy efficiency characteristics and level of heat consumption. Others include the length and diameter of pipelines, environmental conditions, the number of loops and their characteristics.

It has been established that demand management using heat accumulators is a good method of managing district heating. It clearly has investment attractiveness and contributes to the decarbonization of urban areas.

Various works show that such benefits can be achieved:

- reduce peak load by up to 30%,
- significantly reduce harmful emissions and fuel consumption by up to 10%.

Long-term transformation of energy should be aimed at the development of existing and creation of new functional properties of energy system and its elements, which to the greatest extent ensure the achievement of these key values; heating network (all its elements) is considered as the main object of formation of new technological basis, which provides an opportunity to significantly improve the achieved and create new functional properties of energy system.

Comparative characteristic of functional properties of modern energy system and system based on Smart Grid concept demonstrates that Smart Grid implementation means creation of smart

distribution network [8]. This allows against the background of aging of fixed assets and increase in consumption volumes, to achieve an increase in profitability, reliability and failure-free operation while reducing losses of heat and coolant in the networks. In addition, these systems are aimed at improving operational efficiency, optimization and distribution of load on the heating network. Implementation of the Smart Grid concept is innovative and reflects the transition to a new technological paradigm in the energy sector and economy in general, and strengthens energy independence.

Figure 3 summarizes the proposals of energy-saving innovations for district heating companies. At the level of use of fuel and energy resources it is a transition to the multifuel balance. At the level of generation of heat, cold and electricity it is a wide use of alternative and renewable sources. In the transportation of coolant the use of storage of heat and cold, targeted dosed supply of heat or cold to the consumer through mobile heat accumulators and maximum reduction of heat losses.

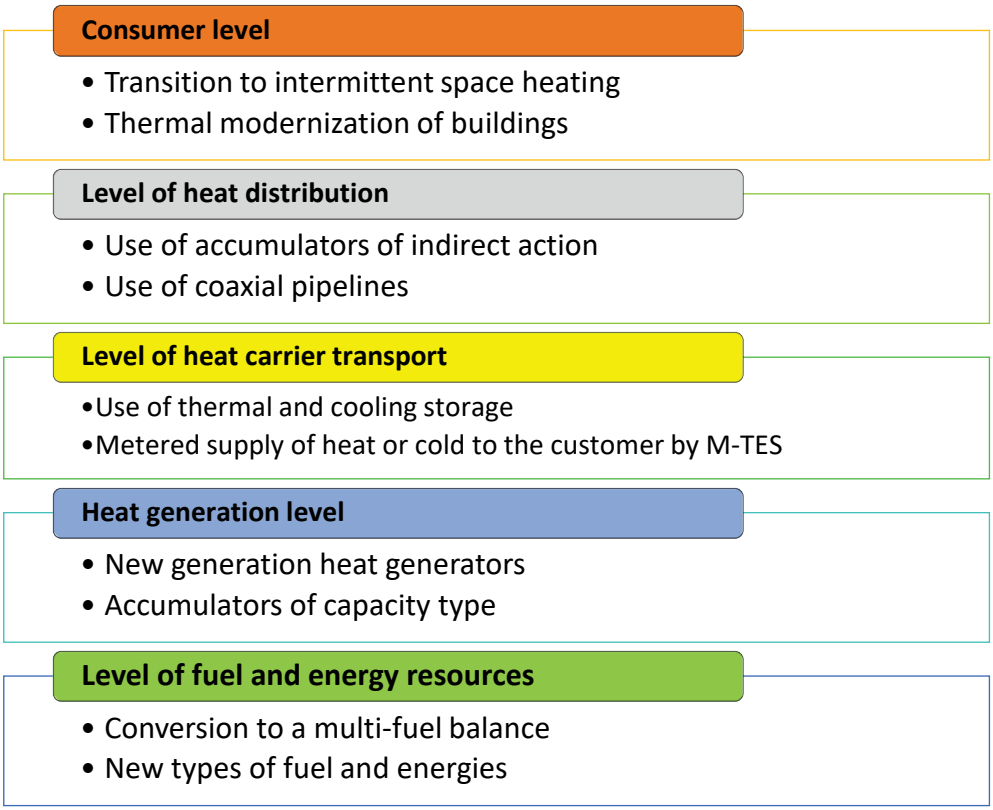

FIGURE 3. *Suggestions for energy saving innovations for district heating companies*

When distributing the heat it is a quantitative-qualitative regulation, the use of a new method of transporting the coolant by coaxial pipelines, developed in the laboratory of heat processes and technologies of the ITTF of the NASU.

It is assumed that the consumer coolant supply pipeline is located inside another pipeline. The return coolant returns to the heat source through the intertube space [9].

Coaxial pipelines proposed for implementation can reduce heat losses almost 2 times and 2 times cheaper than traditional two-pipe heat networks for new construction and modernization of heating networks.

The advantages of the new method of heat carrier transportation are:

- considerable reduction of costs for heat network construction;
- possibility to use existing pipelines in the modernization of the networks;
- decrease of insulation layer thickness and heat losses reduction;

- a smaller length due to a reduction in the number (or even absence) of U-shaped compensators;
- hydraulic stability during operation;
- reduced temperature and pressure drop on network structures;
- a long operational life.

At consumer level, it is proposed, apart from the thermo-modernization of buildings, a transition to intermittent heating of rooms, i.e. heating only when people are permanently inside and a reduction of the temperature at other times.

Application of mobile thermal storage M-TES

One promising direction is the use of the system of storage and mobile transport of thermal energy [10]. Since 2014, research work devoted to mobile thermal energy storage for the disposal and use of industrial waste and excess heat for distributed users has been carried out abroad, and the first commercial projects have been implemented.

Selected examples of such solutions are listed below.

Marco Deckert et al. (Germany), tested a system of two 20-foot tanks filled with sodium acetate trihydrate. The tested M-TES stores up to 2.0 MW/h of heat.

Weilong Wang (Taiwan) investigated direct and indirect heating water storage tanks filled with erythritol – a sugar alcohol characterized by a melting point of 118°C.

Andreas Krönauer et al. (Germany) presented the results of annual tests in which M-TES in the form of a tank filled with 14.0 tons of zeolite and has a heat storage capacity of 2.3 MW/h. The tank uses air as the heating/cooling medium.

In 2020 the authors' group of the laboratory "Processes and Technologies of Heat Supply" of the ITTF of the National Academy of Science of Ukraine created, tested and studied the prototype of mobile heat accumulator with heat capacity 1.2 MW/h (Fig. 4).

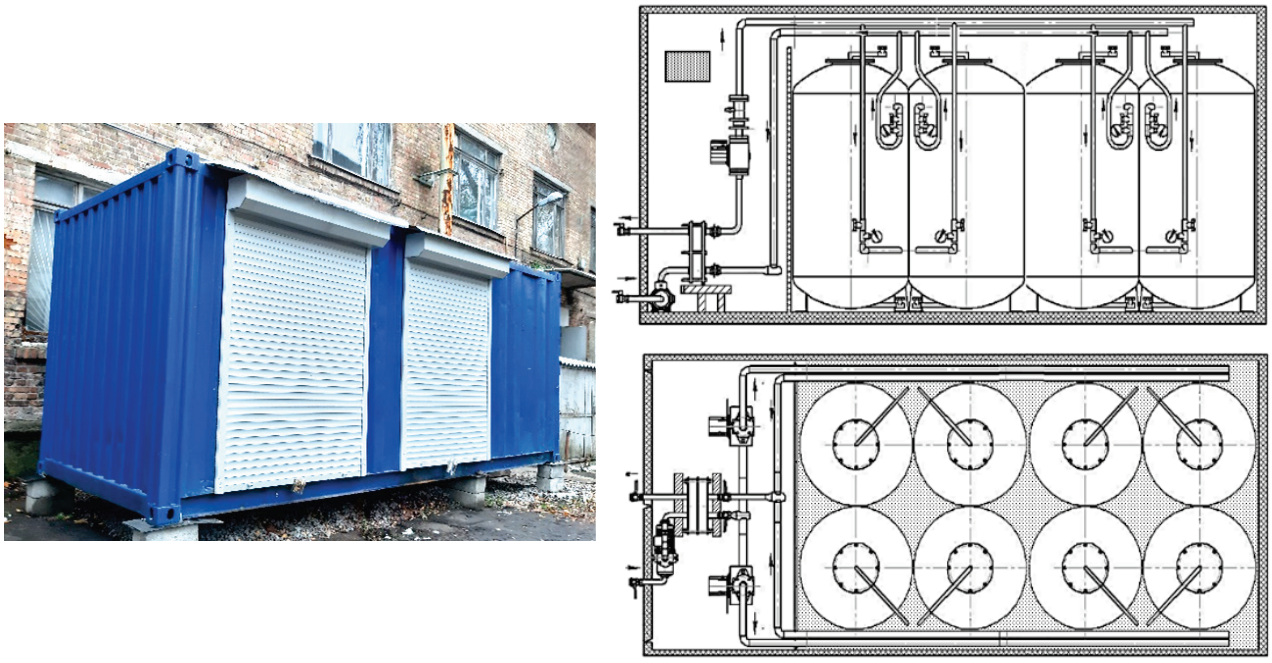

FIGURE 4. *Mobile heat storage MTA-0.5 MW*

Charging time is 4-6 hours, discharging time 10-12 hours, heat storage capacity 200 kW/h, average load power 120 kW, average discharge power 90 kW. The mobile container-type M-TES is equipped with a block heating opinion and heat storage tanks.

For the first time to solve this problem, a design of mobile thermal accumulator is proposed, which is a dry cargo container with an individual heat opinion and mounted tanks-storage of a special design. Feature of such a tank- storage is that its design can solve the problem of stratification, by using a thermal core and substances with a phase transition. As a result of the work for the first time justified and laboratory researched a mixture of functional hydrogels to create an original formula accumulating pseudo-plasticity.

The proposed abandonment of the traditional pipeline transport of heatcarrier and the creation of a fundamentally new discrete heating system. The use of M-TES makes it possible to build a flexible heat scheme for modernization and construction of new heat supply sources. And also to attract local fuels, secondary resources and renewable energy sources to the energy sector.

Conclusions

Global trends in efficiency, energy savings and security of energy systems actualize the task of developing energy storage technologies.

Thermal energy storage can be used to control the heating system load, i.e. to equalize the load on the energy generation source to provide peak heat demand with a high coefficient of equipment capacity utilization. The paper considers the actual technologies of storage and accumulation of thermal energy, which can be used in central heating systems and draws conclusions about the feasibility of their use.

Conflicts of Interest: The author declares no conflict of interest.

References

[1] European Commission. The European green deal: communication from the commission to the European Parliament the European Council, the Council, the European Economic and Social Committee and the Committee of the Regions, 2019, URL: https://eur-lex.europa.eu/legal-content/EN/TXT/uri¼CELEX:52019DC0640.

[2] European Commission “An EU Strategy on Heating and Cooling,” Brussels 2016, available: https://ec.europa.eu/transparency/regdoc/rep/1/2016/EN/1-2016-51-EN-F1-1.PDF.

[3] Union European. EU Energy in figures: Statistical pocketbook 2020, URL: https://op.europa.eu/s/oIDP.

[4] Thermal networks, DBN B.2.5-39: 2008, Valid from 2009-01-07.

[5] Poredos A., Kitanovski A., *District heating and cooling for efficient energy supply*, International Conference on Electrical and Control Engineering, 2011, http://dx.doi.org/10.1109/ICECENG.2011.6058201.

[6] Mathiesen D.A., Averfalk B.V., Werner H., Lund S., Lund H., *Heat Roadmap Europe: Largescale electric heat pumps in district heating systems*, Energies, Review 10(4), https://doi.org/10.3390/en10040578.

[7] Demchenko V., Konyk A., *Main aspects of heat storage processes*, Scientific Works, 84(1), 2020, pp. 48-53, https://doi.org/10.15673/swonaft.v84i1.1868.

[8] Vakulenko I.A., Kolosok S.I., *Connections SMART GRIDS concept with updates of Ukrainian heat power*, Visnyk of Sumy State University Economy, 1, 2019, pp. 14-18, https://doi.org/10.21272/1817-9215.2019.1-2.

[9] Demchenko V.G., Dunyak O.V., Yevtushenko O.V., *Comparative evaluation of the effectiveness of the system of transport of heating carrier based on coaxial tubes*, Thermophysics and Thermal Power Engineering, 38(5), 2016, pp. 39-47, https://doi.org/10.31472/ihe.5.2016.07.

[10] Demchenko V.H., Konyk A.V., *Application of special multifunctional transportable capacitive type terhmo energy storage*, Collection of Abstracts of the XX Scientific and Technical Conference, Chernihiv “Creation and modernization of armaments and military equipment in modern conditions”, 2020, pp. 74-75.

Boris BASOK[1]
Boris DAVYDENKO[1]
Anatoliy PAVLENKO[2]
Vladimir NOVIKOV[1]
Marina NOVITSKA[1]

[1] *Institute of Engineering Thermophysics National Academy of Sciences of Ukraine;*

[2] *Kielce University of Technology, Poland*

Corresponding author: nvg52@i.ua

DOI: 10.53412/jntes-2021-1.2

THE INFLUENCE OF GEOMETRIC CHARACTERISTICS OF THE BUILDINGS FACADES ON THE HEAT TRANSFER TO THE WIND FLOW

Abstract: *This paper presents the results of a numerical study of heat transfer from the external surfaces of freestanding structures in the surface layer of the atmosphere. Numerical models of structures have the same heat transfer area, but different heights and lengths. Numerical modeling of heat transfer from structures in a wind flow in a three-dimensional formulation made it possible to establish some features of convective heat transfer from enclosing structures, depending on the height of the building and the speed of the wind flow. In particular, it is shown that the dependence of the surface-averaged values of the heat flux density on the height of the building has a local minimum, after which the average heat flux density increases insignificantly with an increase in the height of the building.*

Keywords: *CFD modeling, convective heat transfer, heat transfer coefficient, wind flow.*

Introduction

New materials, technologies and architectural solutions in construction can reduce energy consumption during their operation by 50-75% compared to 2000 levels, and the refurbishment of existing residential and industrial installations can still reduce energy consumption by 30% [1]. Together, this will significantly reduce energy costs, make a significant contribution to reducing environmental impact and climate change, and improve indoor climate conditions.

Indeed, energy efficiency can be compared to an untapped clean energy resource with enormous potential. The availability of this resource is associated not so much with technological constraints and existing approaches as with ineffective management.

Decision-making inefficiencies are especially relevant at the early design stage in the case of new construction and at the stage of choosing renovation options in the case of existing buildings. The correct choice of options for architectural solutions for new construction or reconstruction options, as well as effective management after completion of construction can provide modern modeling, in particular, simulation of heat and mass transfer processes in buildings and structures in interaction with the environment.

An important tool in the design and operation of buildings are programs for modeling the energy consumption of buildings [2]. These programs combine many mathematical and empirical models to describe the associated energy flow processes in buildings.

The paper [2] analyzes seven programs for modeling energy consumption of buildings: ESP-r, EnergyPlus, IES, IDA, TAS, TRNSYS and SUNREL. ESP-r is an open software code for building energy simulation developed by the University of Strathclyde (Glasgow – Scotland). ESP-r simulates the thermal, visual and acoustic performance of a building, and estimates the thermal and electrical power of the simulated building.

EnergyPlus software code is a collection of many software modules that estimate the amount of energy required to heat and cool a building using various systems and energy sources.

IDA Indoor Climate and Energy (IDAICE) is a software code for dynamic multi-zone modeling and is intended for a fairly accurate assessment of the thermal indoor climate in individual zones of the structure, as well as the energy consumption of the entire building as a whole.

TasEngineering is designed for dynamic modeling and thermal analysis of buildings and structures.

TRNSYS is widely used to model solar equipment and technological solutions, as well as ordinary buildings and structures.

SUNREL is a software for simulating the energy consumption of small buildings.

These programs combine many fundamental and empirical models to describe a variety of energy flow processes in buildings [1].

This paper examines the process of convective heat transfer between the external surfaces of buildings and the environment. In most cases, the convective heat exchange of building facades with the environment is estimated by calculating the value of convective heat transfer coefficients (CHTC):

$$\alpha_k = \frac{q_s}{T_s - T_a} \tag{1}$$

where:

q_s – the heat flux density on the surface of the surrounding structures;

T_s – temperature of the outer surface of the building;

T_a – ambient temperature.

The more accurately the values of the heat transfer coefficients are determined, the more accurate will be the assessment of the heat taken from the building envelope.

In works [2, 3], an analysis of a significant number of existing empirical models for assessing the CHTC of enclosing structures is carried out. It is shown that all models can be divided into several groups:

Linear equations for convective heat transfer coefficients:

$$\alpha_k = A + B \cdot U \tag{2}$$

where:

A, B – empirical coefficients;

U – wind speed.

Power function of the convective heat transfer coefficient from wind speed:

$$\alpha_k = a + b \cdot U^n \tag{3}$$

where:

a, b, n – empirical coefficients.

Traditional criterion equations:

$$Nu = aRe^b Pr^c + d \quad (4)$$

In total, these works analyzed and classified 76 dependences of the CHTC for the facades of buildings and structures, and most of these relationships are used in the above software packages for modeling the thermal state of buildings.

The indicated correlation for the convective heat transfer coefficients allow one to take into account a number of factors that determine the convective heat flow from the facades of buildings located in the wind flow:

- wind speed;
- wind direction in relation to the orientation of the facades (angle of attack of the wind);
- orientation of the surface relative to the wind in a qualitative sense (windward, leeward);
- the angle of inclination of the surface in relation to the plane of the earth (in extreme cases, horizontal and vertical);
- terrain type;
- shelter by nearby buildings;
- surface texture;
- difference between surface and air temperatures (Δt);
- surface size and aspect ratio.

At the same time, the type of building (high, medium or low rise) and its geometry are also important factors in assessing convective heat loss. However, these factors are not included in the above list, since none of the models for CHTC described in reviews [2, 3] are able to account for differences in the type and geometry of the building. You can also add that relations (2)-(4) take into account the wind speed and one of the above factors, while CFD modeling makes it possible to take into account in one model almost all parameters affecting the convective heat exchange of buildings with the environment, including the factors listed above.

A fairly successful attempt to link the heat transfer of building facades with their geometry was made in [4, 5]. In these studies, 3D CFD modeling of three groups of buildings was carried out. The first group includes buildings, the height of which is $H \le B$ (B is the width of the building) Figure 1, to the second group – buildings with $H \ge B$, and to the third – those with $H = B$. In these works, the building length L remained constant.

As a result, for the windward facades of buildings (in this case, it is a facade $H \times B$), power-law functions (3) of the dependence of CHTC on the wind speed are obtained. In this simulation, the wind speed varied from 1 m/s to 5 m/s at the height of the weather vane, and the temperature difference $T_s - T_a$ (formula (1)) remained constant: T_s = 30°C and T_a = 10°C, which may correspond to the conditions of a cloudless days in the month of April.

In this regard, the main goal of this work is to find out the correlation between the main architectural features of buildings and structures with the boundary convective heat fluxes on the facades of buildings in a wind flow using three-dimensional CFD modeling.

Geometric model

In this paper, models of detached buildings are considered Figure 1. In total, 6 models of buildings were created, interconnected by the condition that the area of the facades of buildings in the environment is the same. The height of buildings H varies, and its length L, the width of buildings B remains constant Figure 1.

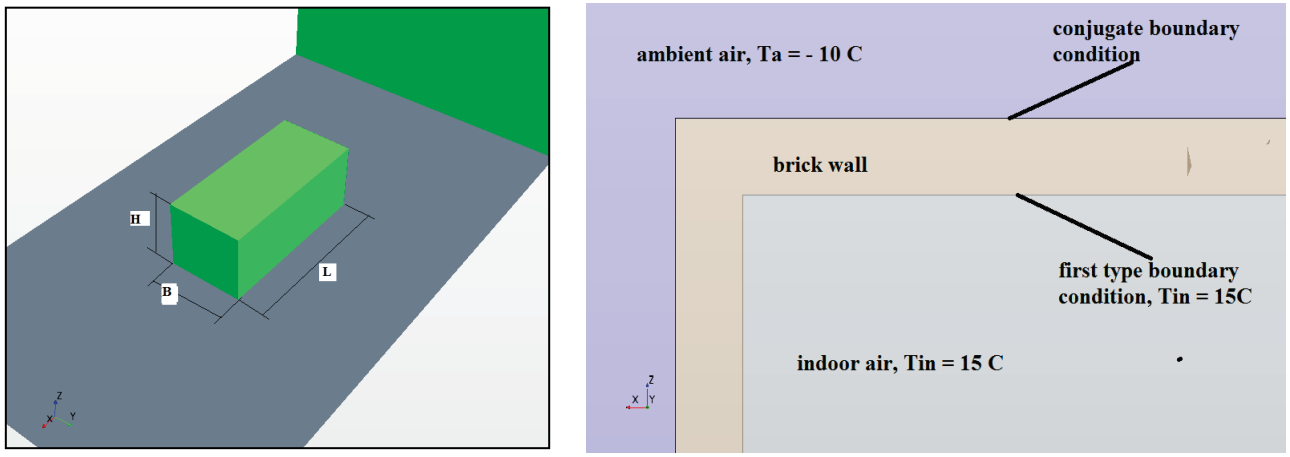

a) b)

FIGURE 1. *Geometricmodelofresearchobjects: a) solution domain; b) fragment of a plane vertical section*

Table 1 shows the calculations of the corresponding dimensions in the building models.

TABLE 1. *Calculation of geometric parameters of CFD models*

Width *B*, m	18	18	18	18	18	18
Length *L*, m	60	50	40	30	20	10
Height *H*, m	10	12.79	16.55	21.88	30.00	43.93
Area of facades, m²	2640	2640	2640	2640	2640	2640

It is assumed that the buildings, the dimensions of which are given in Table 1, have brick walls with a thickness of 30 cm (Fig. 1b).

Constraints, boundary and initial conditions

In accordance with the simulation conditions, detached buildings are located in a turbulent wind flow of the surface layer of the atmosphere under conditions of normal air stratification, the thermophysical characteristics of which are constant.

The computational domains were determined in accordance with the recommendations [6]. At the entrance to the solution area, vertical profiles of the average horizontal wind speed U (logarithmic law), turbulent kinetic energy (k – m^2/s^2) and dissipation rate of turbulent kinetic energy (ε – m^2/s^3) are set, according to the $k-\varepsilon$ turbulence model for atmospheric boundary layer [7]. This model is built for a neutral atmospheric boundary layer in which turbulence occurs only due to friction and shear, and not due to thermal stratification.

$$U(z)=\frac{u^*}{k}\ln\left(\frac{z+z_0}{z_0}\right)$$
$$k(z)=u^{*2}/\sqrt{C_\mu} \qquad (5)$$
$$\varepsilon(z)=\frac{u^{*3}}{k(z+z_0)}$$

where:

u^* – the friction velocity of the atmospheric boundary layer, m/s;

k – Karman constant, 0.41;

z – height above the ground, m;

z_0 – height of the aerodynamic roughness (m) of the terrain type.

The friction speed u^* is related to the wind speed U_{10} at the height of the weather vane (10 m). In this study: U_{10} = 1, 3, 5 and 10 m/s. The z_0 parameter is 1 m, which corresponds to a city center without sufficiently tall buildings [8]. The wind speed vector is directed perpendicular to the windward surface of the building facade. The incident air temperature is −10°C, which is taken as the incident air temperature T_a in equation (1). The constant temperature assumption over the height of the atmospheric boundary layer is a good enough assumption for neutral air stratification with zero heat flux at the ground and a limited height of the solution region. The temperature on the inner surface of building fences is considered to be set (+15°C). On the outer surfaces of the building fences, the conditions for conjugation of the temperature and heat flux fields are set.

Mesh models

In this CFD study, several mesh models were used: rectangular uniform mesh Figure 2a, rectangular mesh with a seal at the facades surfaces Figure 2b, and mesh with polyhedral cells Figure 2c.

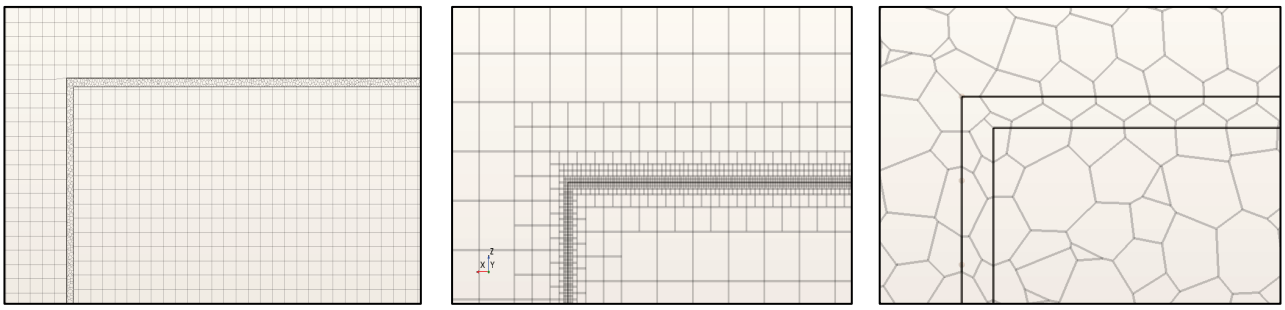

a) b) c)

FIGURE 2. *Mesh models in numerical study*

The defining size in all mesh models corresponded to 0.5 m, and the number of cells varied from 2400 to 4000 thousand cells. Analysis of the sensitivity of the solution to mesh models and to the number of cells in the models did not give significant deviations. The largest deviation was no more than 3%.

Mathematical model

The system of equations describing hydrodynamics and heat transfer in the system under study consists of:

- ContinuityEquations:

$$\frac{\partial \rho}{\partial \tau}+\frac{\partial(\rho u)}{\partial x}+\frac{\partial(\rho v)}{\partial y}+\frac{\partial(\rho w)}{\partial z}=0 \tag{6}$$

- Navier-Stokes System of Equations:

$$\frac{\partial \rho u}{\partial \tau}+\frac{\partial\left(\rho u^2\right)}{\partial x}+\frac{\partial(\rho u v)}{\partial y}+\frac{\partial(\rho u w)}{\partial z}= =-\frac{\partial p}{\partial x}+2\frac{\partial}{\partial x}\left[\mu_{ef}\frac{\partial u}{\partial x}\right]+\frac{\partial}{\partial y}\left[\mu_{ef}\left(\frac{\partial u}{\partial y}+\frac{\partial v}{\partial x}\right)\right]+\frac{\partial}{\partial z}\left[\mu_{ef}\left(\frac{\partial u}{\partial z}+\frac{\partial w}{\partial x}\right)\right] \tag{7}$$

$$\frac{\partial \rho v}{\partial \tau}+\frac{\partial(\rho v u)}{\partial x}+\frac{\partial\left(\rho v^{2}\right)}{\partial y}+\frac{\partial(\rho v w)}{\partial z}= \\ =-\frac{\partial p}{\partial y}+\frac{\partial}{\partial x}\left[\mu_{ef}\left(\frac{\partial v}{\partial x}+\frac{\partial u}{\partial y}\right)\right]+2\frac{\partial}{\partial y}\left[\mu_{ef}\frac{\partial v}{\partial y}\right]+\frac{\partial}{\partial z}\left[\mu_{ef}\left(\frac{\partial v}{\partial z}+\frac{\partial w}{\partial y}\right)\right] \tag{8}$$

$$\frac{\partial \rho v}{\partial \tau}+\frac{\partial(\rho v u)}{\partial x}+\frac{\partial(\rho w v)}{\partial y}+\frac{\partial\left(\rho w^{2}\right)}{\partial z}= \\ =-\frac{\partial p}{\partial z}+\frac{\partial}{\partial x}\left[\mu_{ef}\left(\frac{\partial w}{\partial x}+\frac{\partial u}{\partial z}\right)\right]+\frac{\partial}{\partial y}\left[\mu_{ef}\left(\frac{\partial w}{\partial y}+\frac{\partial v}{\partial z}\right)\right]+2\frac{\partial}{\partial z}\left[\mu_{ef}\frac{\partial w}{\partial z}\right]-\rho g \tag{9}$$

- Energy Equation:

$$\frac{\partial\left(C_{p}\rho T\right)}{\partial \tau}+\frac{\partial\left(C_{p}\rho u T\right)}{\partial x}+\frac{\partial\left(C_{p}\rho v T\right)}{\partial y}+\frac{\partial\left(C_{p}\rho w T\right)}{\partial z}= \\ =\frac{\partial}{\partial x}\left[\lambda_{ef}\frac{\partial T}{\partial x}\right]+\frac{\partial}{\partial y}\left[\lambda_{ef}\frac{\partial T}{\partial y}\right]+\frac{\partial}{\partial z}\left[\lambda_{ef}\frac{\partial T}{\partial z}\right] \tag{10}$$

- Ideal gas equation of state:

$$p=\rho R T \tag{11}$$

Air flows in the surface layer of the atmosphere are traditionally modeled by numerically solving the Reynolds-averaged system of Navier-Stokes differential equations, which is closed by two additional equations for the kinetic energy of turbulence (12) and dissipation of the kinetic energy of turbulence (13):

$$\frac{\partial \rho k}{\partial \tau}+\frac{\partial \rho u k}{\partial x}+\frac{\partial \rho v k}{\partial y}+\frac{\partial \rho w k}{\partial z}= \\ =\frac{\partial}{\partial x}\left[\left(\mu+\frac{\mu_{t}}{\sigma_{k}}\right)\frac{\partial k}{\partial x}\right]+\frac{\partial}{\partial y}\left[\left(\mu+\frac{\mu_{t}}{\sigma_{k}}\right)\frac{\partial k}{\partial y}\right]+\frac{\partial}{\partial z}\left[\left(\mu+\frac{\mu_{t}}{\sigma_{k}}\right)\frac{\partial k}{\partial z}\right]+\mu_{t}S^{2}-\rho\varepsilon \tag{12}$$

$$\frac{\partial \rho \varepsilon}{\partial \tau}+\frac{\partial \rho u \varepsilon}{\partial x}+\frac{\partial \rho v \varepsilon}{\partial y}+\frac{\partial \rho w \varepsilon}{\partial z}= \\ =\frac{\partial}{\partial x}\left[\left(\mu+\frac{\mu_{t}}{\sigma_{\varepsilon}}\right)\frac{\partial \varepsilon}{\partial x}\right]+\frac{\partial}{\partial y}\left[\left(\mu+\frac{\mu_{t}}{\sigma_{\varepsilon}}\right)\frac{\partial \varepsilon}{\partial y}\right]+\frac{\partial}{\partial z}\left[\left(\mu+\frac{\mu_{t}}{\sigma_{\varepsilon}}\right)\frac{\partial \varepsilon}{\partial z}\right]+C_{1}\frac{\varepsilon}{k}\mu_{t}S^{2}-C_{2}\rho\frac{\varepsilon^{2}}{k} \tag{13}$$

where:

$$S=\left[\left(\frac{\partial u}{\partial y}+\frac{\partial v}{\partial x}\right)^{2}+\left(\frac{\partial v}{\partial z}+\frac{\partial w}{\partial y}\right)^{2}+\left(\frac{\partial w}{\partial x}+\frac{\partial u}{\partial z}\right)^{2}+2\left(\frac{\partial u}{\partial x}\right)^{2}+2\left(\frac{\partial v}{\partial y}\right)^{2}+2\left(\frac{\partial w}{\partial z}\right)^{2}\right]^{0.5}$$

It is shown in [9] that in this case, for the problems of turbulent transport in atmospheric flows over the underlying surface, it is advisable to use the following constants for the k – ε model: C_{μ} = 0.033; σ_{k} = 1.0; σ_{ε} = 1.3; $C1_{\varepsilon}$ = 1.176; $C2_{\varepsilon}$ = 1.92.

Heat transfer in solids (enclosing structures) is described by the heat conduction equation:

$$C_p \rho_m \frac{\partial T}{\partial \tau} = \frac{\partial}{\partial x}\left[\lambda_m \frac{\partial T}{\partial x}\right] + \frac{\partial}{\partial y}\left[\lambda_m \frac{\partial T}{\partial y}\right] + \frac{\partial}{\partial z}\left[\lambda_m \frac{\partial T}{\partial z}\right] \quad (14)$$

In modern CFD packages, such as ANSYS or STAR CCM, the above system of equations is solved numerically according to explicit, implicit or mixed schemes.

Results

Numerical integration of the system of equations (6)-(14) using CFD packages allows calculating all field functions for unambiguous determination of both local and average values of the thermal characteristics of the simulated object.

Figure 3 shows the average values of the boundary heat flux q_s over the surfaces of all facades, depending on the building height H and the wind flow rate U_{10}. The data indicate that with an increase in wind speed, the value of the heat flux increases. In the range of building heights from H = 10 m to H = 16 m, a decrease in the average heat flux with increasing height is observed, and with a further increase in the height H at all wind speeds, a slow increase in q_s is observed.

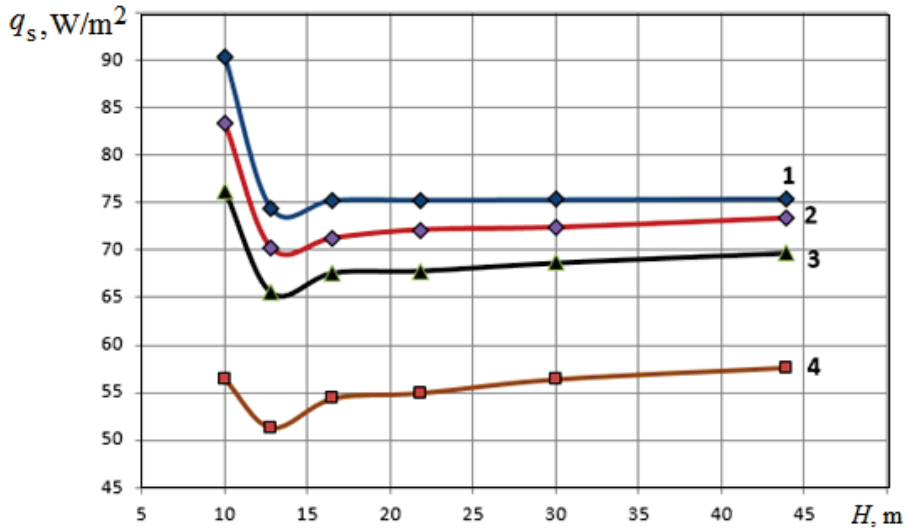

FIGURE 3. *Average heat flux qs on the surface of buildings depending on the height of the building and wind speed: 1 – U_{10} = 10 m/s; 2 – 5 m/sec; 3 – 3 m/s; 4 – 1 m/sec*

The graphs in Figure 3 clearly indicate that the height of the building affects the convective heat transfer of structures.

Heat transfer coefficient

In modern governing documents of architecture and construction, the convective component of the heat flux on the outer surfaces of the enclosing structures is proposed to be estimated by means of the heat transfer coefficients, which are regulated in these documents. Therefore, the authors of most of the works devoted to the thermal characteristics of buildings and structures pay particular attention to this coefficient. CFD modeling allows to numerically determine the fields of velocity, temperature, heat fluxes and other field functions, allowing to calculate both local and average values of heat transfer coefficients on the facades of the buildings under study.

In Figures 4-6 show the local values of the heat transfer coefficients on the outer surfaces of the enclosing facades of the simulated buildings. Local coefficients are calculated along centerlines on roof surfaces, windward and leeward facades.

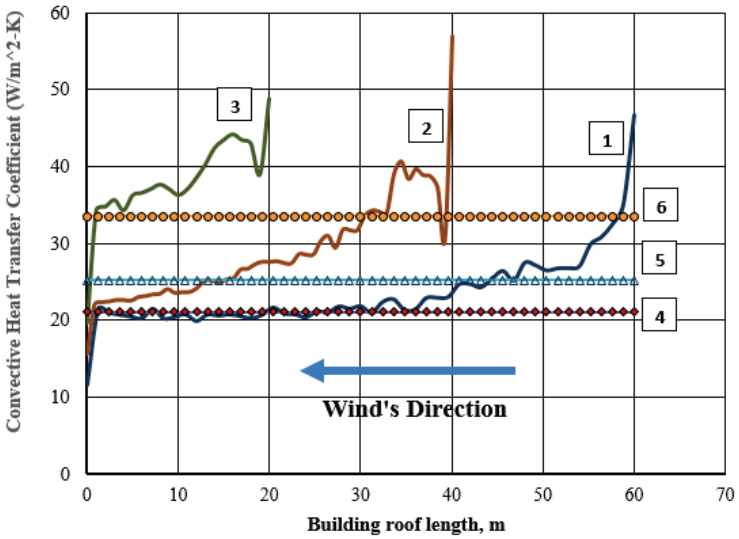

FIGURE 4. *Values of heat transfer coefficients on roofs of buildings of different heights: 1 – corresponds to a building with a height of H = 10 m; 2 – H = 16 m; 3 – H = 30 m; 4 – Frank's model; 5 – McAdams model; 6 – polynomial model*

An increase in the values of local heat transfer coefficients on the roof of buildings with an increase in its height (curves 1, 2, 3 in Figure 4) is due to an increase in the wind flow velocity with an increase in the distance from the ground.

As expected, the local heat transfer coefficients on the windward facade of buildings are rather much higher than the corresponding values on the leeward side Figures 5 and 6. Moreover, the higher the building, the greater the difference. See also Figures 5 and 6 indicate that the values of the heat transfer coefficients on the windward and leeward sides of the building do not actually depend on its height. At the ground, the coefficients coincide, and as the height increases, the coefficients correlate quite well in physical values up to the separation of the wind flow at the edge of the buildings.

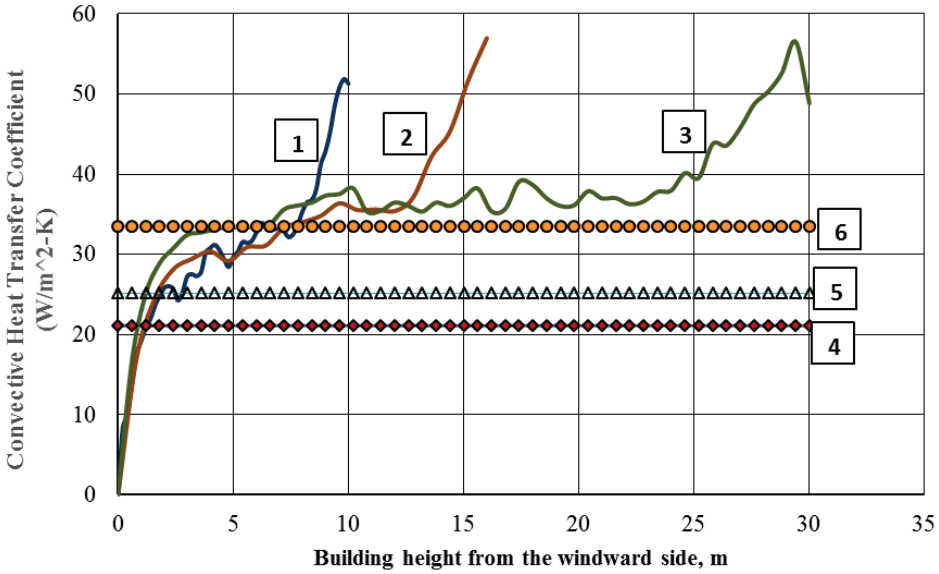

FIGURE 5. *Values of heat transfer coefficients on the windward side of buildings of different heights: 1 – corresponds to a building with a height of H = 10 m; 2 – H = 16 m; 3 – H = 30 m; 4 – Frank's model; 5 – McAdams model; 6 – polynomial model*

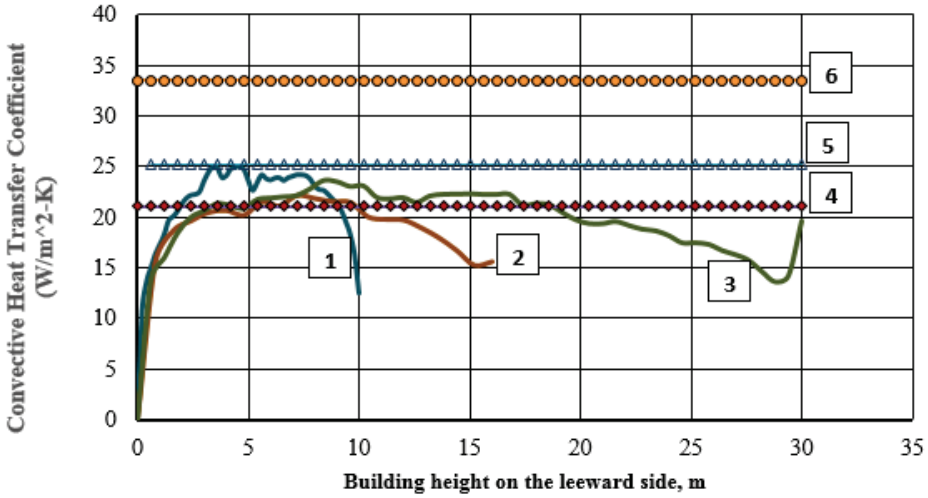

FIGURE 6. *Values of heat transfer coefficients on the leeward side of buildings of different heights: 1 – corresponds to a building with a height of H = 10 m; 2 – H = 16 m; 3 – H = 30 m; 4 – Frank's model; 5 – McAdams model; 6 – polynomial model*

Comparison of known models for heat transfer coefficients with simulation data

In Figures 4-6 show a comparison of local values of heat transfer coefficients for buildings with different geometries with known calculation models for average values of heat transfer coefficients, which are used in the above-mentioned software packages for calculating the thermal characteristics of new buildings and buildings in need of renovation.

It should be noted that the models below, which are Frank, McAdams and the polynomial model, were chosen almost arbitrarily, since in the works known to us [2, 3, 10], no preference is made for any of them:

Frank's formula [10]:

$$\alpha_k = 7.34U^{0.656} + 3.7e^{-1.97U} \tag{15}$$

The second term on the right-hand side of formula (15) characterizes the amount of heat transfer by natural convection. For the calculated wind speed for winter conditions, the average speed is taken from those points for January, the frequency of which is 16% or more.

McAdams model [2, 3]:

$$\alpha_k = 5.687\left[m + n\left(\frac{U_f}{0.3048}\right)^p\right] \tag{16}$$

where *m, n, p* are roughness parameters for smooth and rough surfaces [2, 3].

Polynomial model [2, 3]:

$$\alpha_k = D + EU_{10} + FU_{10}^2 \tag{17}$$

where:

α_k – combined emissivity and convection coefficient;

D, E, F – roughness coefficients [2, 3].

Comparison of local values of heat transfer coefficients on external surfaces of buildings obtained as a result of this CFD simulation with the data of empirical models for average coefficients indicates that none of the considered empirical models coincides with local calculated data.

However, we can say that Frank's model (curve 4 in Figure 6) more or less corresponds to local CHTC on the roofs of low buildings (no more than 10 m). Other considered models are not suitable for use in

assessing convective heat fluxes on the roofs of buildings and structures. The polynomial model fairly closely describes convective heat transfer from the windward side, while the Frank and McAdams models correlate with heat transfer on the leeward side of the models. It is quite possible that other models of convective heat transfer will be more adequate.

Influence the wind flow speed on the value of the heat transfer coefficient on the building facades

In specialized software codes for assessing the thermal state of buildings, which were discussed above, the convective component of heat fluxes is calculated using heat transfer coefficients averaged over the surfaces of the enclosing structures [2, 3]. Also, the average values of the heat transfer coefficients are regulated in the management documents of architecture and construction known to us. In particular, Ukraine has adopted a standard for the convective heat transfer coefficient for the external surfaces of building envelopes, corresponding to a value of 23 W/m²K.

The results of CFD modeling of buildings of different heights with the same heat transfer surface at four values of wind speed are used to obtain a correlation between the value of the average CHTC over the surfaces of buildings and the average speed of the wind flow U_{10} at the height of the weather vane (10 m).

In Figure 7 shows the graphs of the dependences of the CHTC from the height of the buildings and the speed of the wind flow. The graphs unambiguously indicate that the convective component of the heat flow from the external facades of buildings significantly depends from their height and the speed of the wind flow.

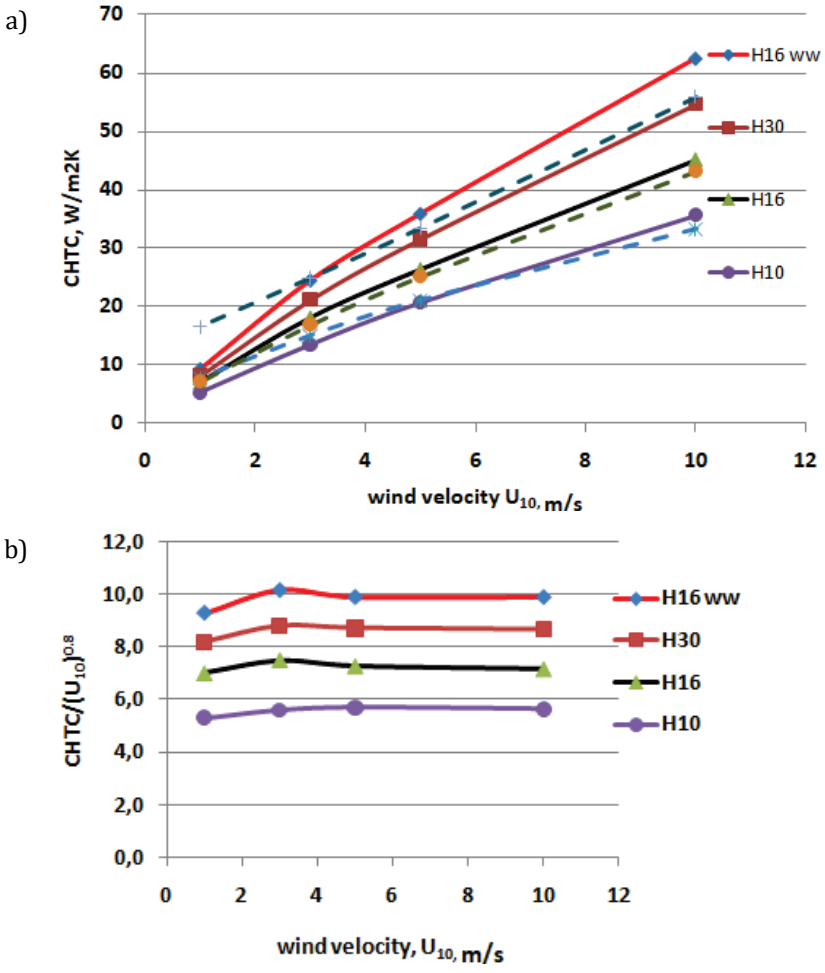

FIGURE 7. *Profiles of surface-averaged CHTC (CHTCavg) on the surface of the heat transfer of buildings: H10, H16, H30 – buildings with a height of 10, 16, 30 m; H16ww – corresponds to the windward side of a 16 m high building; 1 – CHTCavg values according to the polynomial model; 2 – according to the McAdams model; 3 – after Frank's model*

Taking into account the turbulent nature of air movement in the atmosphere, it is advisable to consider the dependence of the ratio $\alpha_k / (U_{10})^{0.8}$ on the wind speed. These dependences are shown in Figure 7b. The horizontal character of the curves in Figure 7b indicates that the functions $\alpha_k = F(U_{10})$ are fairly accurately approximated by power functions of the form (3). Table 2 shows an explicit view of these functions depending on the height of the building, obtained from the results of CFD modeling.

***TABLE 2**. An explicit form of functions $\alpha_k = F(U_{10})$ depending on the height of the building, obtained from the results of CFD modeling*

Building height	H = 10	H = 16	H = 30	Windward facade of the building H = 16 m
CHTCavr	$\alpha_k = 5.6U_{10}^{0.8}$	$\alpha_k = 7.2U_{10}^{0.8}$	$\alpha_k = 8.6U_{10}^{0.8}$	$\alpha_k = 9.8U_{10}^{0.8}$

For comparison, Figure 7a shows the values of the heat transfer coefficients calculated according to known models for estimating α_k. The graphs in Figure 7a show that Frank's model is appropriate for buildings up to 10 m in height, the McAdams model gives good results for buildings up to 16 m in height, and the polynomial model works for buildings 30 m or more.

Conclusion and findings

Based on the results of this study, the following conclusions can be drawn:

Empirical models, such as Frank's formula, designed to assess the convective component on the outer surfaces of the enclosing structures of buildings and structures, take into account only 2, 3 parameters from a large number of factors on which the convective heat exchange of buildings in the wind flow of the atmospheric surface layer depends. Modern CFD modeling packages allow simultaneously taking into account a much larger number of factors affecting convection, including the geometry of buildings and their architectural features. Therefore, when creating sufficiently important objects, it is advisable to use CFD modeling, which is quite convincingly shown by this study.

The results of this numerical simulation clearly indicate that the geometry of buildings and their architectural features affect the convective heat transfer of structures to the environment, which in turn changes the heat balance of buildings as a whole.

Conflicts of Interest: The author declares no conflict of interest.

References

[1] Clarke J.A., *Energy Simulation in Building Design*. 2-nd Edition, Butterworth-Heinemann Linacre House, Jordan Hill, Oxford OX2 8DP 2001, 373 p.

[2] Mirsadeghi M., Cóstola D., Blocken B., Hensen J.L.M., *Review of external convective heat transfer coefficient models in building energy simulation programs: implementation and uncertainty*. Applied Thermal Engineering, March 2013.

[3] Palyvos J.A., *A survey of wind convection coefficient correlations for building envelope energy systems' modeling*, Applied Thermal Engineering, 28 (2008), pp. 801-808.

[4] Montazeri H., Blocken B., Derome D., Carmeliet J., Hensen J.L.M., *CFD analysis of forced convective heat transfer coefficients at windward building facades: Influence of building geometry*. J. Wind Eng. Ind. Aerodyn. 146, 2015, pp. 102-116.

[5] Iousef S., Montazeri H., Blocken B., van Wesemael P., *Impact of exterior convective heat transfer coefficient models on the energy demand prediction of buildings with different geometry*. Building Simulation, 2019, 12(5), pp. 797-816. https://doi.org/10.1007/s12273-019-0531-7.

[6] Franke J., Hellsten A., Schlünzen H., Carissimo B., *Best practice guideline for the CFD simulation of flows in the urban environment*, COST Action 732: Quality assurance and improvement of microscale meteorological models, Hamburg 2007.

[7] Richards P.J., Hoxey R.P., *Appropriate boundary conditions for computational wind engineering models using the k-ε turbulence model*, J. Wind Eng. Ind. Aerodyn. 46-47 (1993), pp. 145-153.

[8] Wieringa J., *Updating the Davenport roughness classification*, J. Wind Eng. Ind. Aerodyn. 41-44(1992), pp. 357-368.

[9] Basok B.I., *Chislennoe modelirovanie vetrovih potokov v zone gorodskoi zastroiki.* Basok B.I., Davidenko B.V. Novikov V.G., Vidnovlyuvalna energetika. 2014, No. 2, 37, s. 46-59.

[10] Fokin K.F., *Stroitelnaja teplotechnika ograzdajushcich castej zdanij*. Moscow «AVOK-PRESS» 2006, 252c.

Mikhail K. BEZRODNY
Natalia PRYTULA
Aleksander ZARUBIN

National Technical University of Ukraine «Igor Sikorsky Kyiv Polytechnic Institute»,
37 Prospekt, Kyiv, 03056, Ukraine

Corresponding author: prytulanatalia88@gmail.com

DOI: 10.53412/jntes-2021-1.3

ENERGY EFFICIENCY OF HEAT PUMP HEAT SUPPLY SYSTEM WITH HEAT UTILIZATION OF TECHNOGENIC AIR EMISSIONS

Abstract: *In this article, the aim is to analyze the conditions of efficient use of heat obtained from the utilization of technogenic air sources, and to find the optimal values of the heat usage parameters in the heat pump heating system. This will allow using the thermal potential, which was previously wasted. It is necessary to determine the optimal degree of cooling of the lower heat source in the evaporator of the heat pump (optimal depth of use of the lower energy source), because with decreasing coolant temperature at the evaporator outlet and increasing the useful effect – proportionally increases the cost of HP compressor.*

Keywords*: efficient use of heat, optimal the heat usage, heat pump, heating system*

Introduction

Industrial units and systems, where the high-temperature heat-technological process is realized, create the technical base of main productions of the national economy, namely ferrous and non-ferrous metallurgy, production of building materials, food industry and mechanical engineering. They consume almost 75-80% of high-potential thermal energy, but the use of thermal energy in these economy productions is characterized by a relatively low fuel heat utilization rate – up to 30%. As a result of technological processes at industrial enterprises there is a large amount of low-temperature thermal energy which is not used in the technological cycle. Depending on specific conditions, the spent thermal energy can be used in heat pumps as a lower heat source for heat supply of workshops, production areas, warehouses of industrial enterprises [1-3].

Thus, through the introduction of heat pumps in enterprises with high–temperature processes and units, it is possible to create a combined energy technology system that naturally connects energy and heat technology systems to ensure the highest economic efficiency of energy production and technological products realization [3].

Almost all scientific or research developments related to the introduction of heat pump technology for technogenic air heat sources recovery are at the stage of individual design solutions and applications. In the available literature there are only isolated studies without comprehension and full analysis of results and attempts to apply them to other systems. Thus, the analysis of research in the field of HP applications in heat supply systems showed that this issue is open and necessary to address [1, 4].

Based on the method of balance equations, a theoretical model of the heat pump system (HPS) for heat supply (Fig. 1), as well as a method of thermodynamic analysis of its work was developed. Using the numerical calculation method, data were obtained that allow to evaluate the efficiency of technogenic sources from the condition of obtaining the maximum useful effect in the heat pump heating system, and determine the optimal depth of technogenic air emissions as a lower energy source.

Description of the basic heat pump heating system working at the expense of utilization of technogenic air sources

Figure 1 shows a HPS heat supply system that works by utilization of technogenic air heat sources.

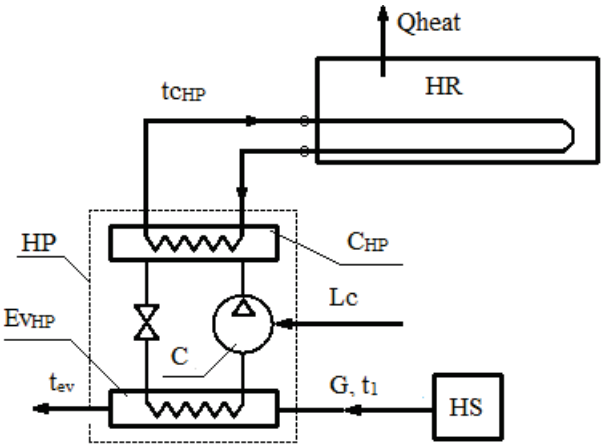

FIGURE 1. *HPS heat supply system that works by utilization of technogenic air heat sources: HR – heated room, HS – heat source, HP – heat pump, C_{HP} – HP condenser, Ev_{HP} – HP evaporator, C – compressor*

The operation principle is a follows: low-temperature heat source, i.e. exhausted air with temperature t_1 (varies in range 20...60°C) and mass flow G_a is fed into the HP evaporator. Here the coolant is cooled and its outlet temperature is t_{ev}. The heated room has heat loss to the environment Q_h. For their compensation the flow extracted from the HP condenser Q_{heat} is used with the temperature of the heating coolant $t_{C_{HP}}$ at the entrance to the heating system.

The temperature of the coolant at the outlet of the heat pump evaporator t_{ev} should be determined from the condition of obtaining the maximum useful effect, because the amount of heat taken from the lower source energy depends on the temperature difference at the inlet and outlet of the HP evaporator, and the consumption of coolant. In this case, the thermal capacity of the HP and the temperature of the coolant in the heating system are known values, which are determined by the characteristics and needs of the object in thermal energy to reach the goals of heat supply.

Thermodynamic analysis of the use of heat from man-made air emissions in the heat pump system for low-temperature heating

The condition of further analysis is the conditions of use of technogenic heat source, which correspond to the maximum useful effect, taking into account energy expenses for the HP compressor drive.

$$Q = Q_{ut} - \frac{L_c}{\eta_{\text{CPP}}\eta_{\text{EPL}}} \tag{1}$$

where:

Q_{ut} – heat flow utilized while cooling of technogenic air emissions, kW;

L_c – energy costs for the drive of the HP compressor, kW;

η_{CPP} – energy efficiency of a condensing power plant, it is taken equal to 0.38;

η_{EPL} – efficiency of power lines, it is taken equal to 0.95 [2].

The heat flux Q_{ut}, that is utilized during the cooling of the exhaust gases is defined as

$$Q_{ut} = Q_{ev} = G_a c_p (t_1 - t_{ev}) \tag{2}$$

where:

Q_{ev} – heat flow in the heat pump evaporator, kW;

G_a – mass flow of technogenic air source, kg/sec;

c_p – specific heat of air, respectively, kJ/(kg°C);

t_1, t_{ev} – the temperature of the technogenic air source at the inlet and outlet of the HP evaporator, respectively, °C.

The energy consumption of the HP compressor L_c is determined by the expression

$$L_к = Q_{ev} / (\varphi - 1) \tag{3}$$

where φ is the actual HP transformation coefficient.

The theoretical heat transformation coefficient of an ideal Carnot cycle can be written as

$$\varphi_{th} = \left[1 - \frac{T_{ev}^{\text{HP}}}{T_c^{\text{HP}}} \right]^{-1} \tag{4}$$

where:

T_{ev}^{HP} – the absolute temperature of evaporation of the refrigerant in the HP evaporator, K;

T_c^{HP} – the absolute condensation temperature of the refrigerant in the HP condenser, K.

The absolute temperature of evaporation of the refrigerant in the HP evaporator is determined as

$$T_{ev}^{\text{HP}} = 273 + t_{ev} - \Delta t_{ev} \tag{5}$$

where Δt_{ev} is the difference in temperature of the coolant and the working fluid of the HP at the outlet of the evaporator HP, °C.

The absolute condensation temperature of the refrigerant in the HP condenser is defined as

$$T_c^{\text{HP}} = 273 + t_c + \Delta t_c \tag{6}$$

where:

t_c – the water temperature at the outlet of the HP condenser, °C;

Δt_c – the temperature difference between the working fluid of the HP and the water at the outlet of the HP condenser, °C.

Substituting (5), (6) into (4), we obtain the expression for determining the Carnot cycle transformation coefficient taking into account thermal irreversibility

$$\varphi_T = \left[1 - \frac{273 + t_{ev} - \Delta t_{ev}}{273 + t_c + \Delta t_c} \right]^{-1} \tag{7}$$

According to the recommendations, we can assume that Δt_{ev} = 10°C for air, respectively, and Δt_c = 5°C for low–temperature water heating system.

However, equation (7) does not take into account the nature of the actual cycle in the heat pump. To take into account various types of irreversibility and the nature of the cycle during the operation of the real HP in (7) is introduced a correction factor, which is the efficiency of HP. Thus, equation (7) for the real cycle of the heat pump unit can be rewritten as

$$\varphi = \eta_{\text{HP}} \left[1 - \frac{273 + t_{ev} - \Delta t_{ev}}{273 + t_c + \Delta t_c} \right]^{-1} \tag{8}$$

where η_{HP} is the efficiency of the heat pump that can be taken 0.6.

To determine the temperature of the coolant supplied from the HP condenser to the low–temperature water heating system, has the force of the equation, which is derived based on the analysis of heat transfer processes in the system heating water – indoor air – atmospheric air

$$t_c = t_r + \left(t_c^{\text{est}} - t_r \right) \left[\left(t_r - t_0 \right) / \left(t_n - t_0^{\text{est}} \right) \right]^{\frac{1}{(1+n)}} \tag{9}$$

where:

t_r – room temperature, °C;

t_0 – ambient temperature, °C;

t_0^{est} – the estimated temperature of the coolant in the heating system, in case of designed ambient temperature t_0^{est} (t_0^{est} = –20°C);

n – coefficient that characterizes the selected heating system (for low–temperature heating systems n = 0).

Taking into account the above formulas (2)-(9), the initial equation (1) can be written as

$$Q = G_a c_p (t_1 - t_{ev}) \left[1 - \frac{1}{(\varphi - 1)\eta_{\text{CPP}} \eta_{\text{EPL}}} \right] \tag{10}$$

Therefore, the specific beneficial effect that can be obtained by utilizing the heat of technogenic air sources using a heat pump, taking into account the energy costs for the drive of the compressor of the heat pump, attributed to 1 kg of air heat source, is determined by the ratio

$$q = \frac{Q}{G_a} = c_p (t_1 - t_{ev}) \left[1 - \frac{1}{(\varphi - 1)\eta_{\text{CPP}} \eta_{\text{EPL}}} \right] \tag{11}$$

The algorithm for obtaining the specific useful effect from the use of technogenic air emissions allows us to investigate the calculation method of the conditions for achieving the maximum value of this useful effect, ie the optimal values of cooling temperature of air emissions at the outlet of the HP evaporator or the optimal degree of heat.

Estimated analysis of the optimal parameters of heat use of technogenic air emissions in the low–temperature heating system

The purpose of the calculation analysis is to implement a numerical calculation according to the above method to determine the optimal conditions for heat utilization of technogenic emissions, namely the optimal cooling temperature t_{ev}^{opt} and its dependence on the parameters of the problem, ie the temperature of technogenic air emissions t_1, estimated temperature of the coolant in the heating system t_c^{est} and ambient temperature t_0.

According to this idea, Figure 2 shows the calculated dependences of the specific useful effect due to the utilization of heat of technogenic air emissions from the emission temperature at the outlet of the HP evaporator for different values of the source temperature (t_1 = 20°C; 30°C; 40°C; 50°C; 60°C), at different values of the calculated temperature of the coolant in the heating system (t_c^{est} = 40°C; 50°C; 60°C) and the estimated ambient temperature (t_0 = –20°C).

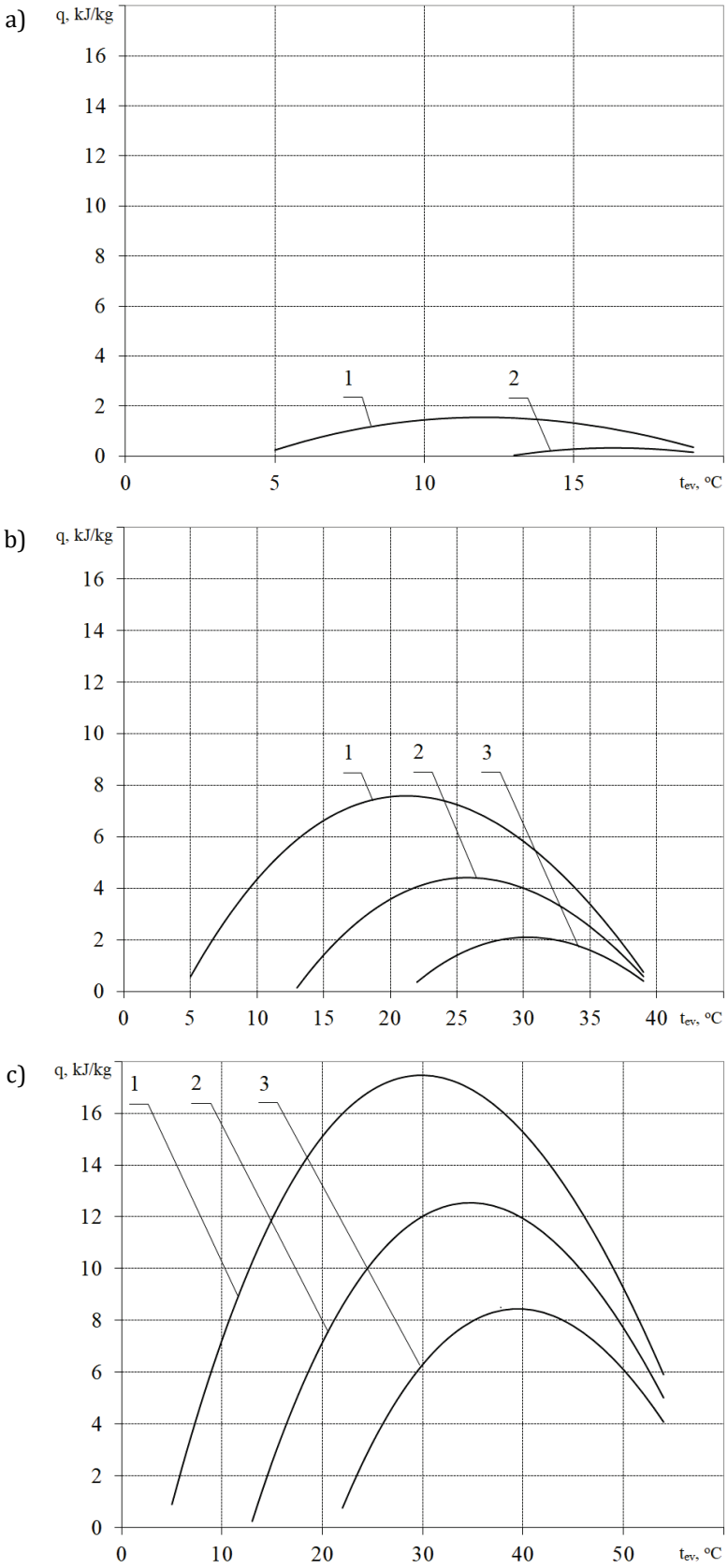

FIGURE 2. *Specific useful effect received as a result of technogenic air heat sources utilization by a HP depending on the temperature at the outlet of the HP evaporator: a), b), c) temperature of technogenic air emissions at the inlet of the HP evaporator* t_1 *= 20 °C; 30 °C; 40 °C; 50 °C; 60 °C respectively: 1-3 – at the design temperature of the heating coolant in the heating system* t_c^{est} *= 40 °C; 50 °C; 60 °C*

As can be seen from the graphs, these dependences are extreme in nature with the maximum useful effect, which corresponds to the optimal values of the exhaust air temperature at the outlet of the HP evaporator. The maximum useful effect increases with increasing temperature of technogenic emissions and with decreasing design temperature of the coolant in the heating system, i.e. under conditions that improve the operating conditions of the heat pump.

The obtained dependences also allow to determine the conditions for achieving the maximum of the useful effect, i.e. the optimal values of the system parameters. Figure 3 shows the dependences of the optimal air temperatures at the outlet of the HP evaporator and the corresponding dependences of the difference in air temperatures at the inlet and outlet of the HP evaporator, which characterize the degree of heat use of technogenic emissions. It is seen that the degree of utilization of heat of air emissions increases (as well as the maximum useful effect) with increasing emission temperature t_1 and with a decrease in the design temperature of the coolant in the heating system t_c^{est}. This is due to the fact that with increasing efficiency of HP conditions improve for deeper utilization of the lower heat source, i.e. the heat of air emissions.

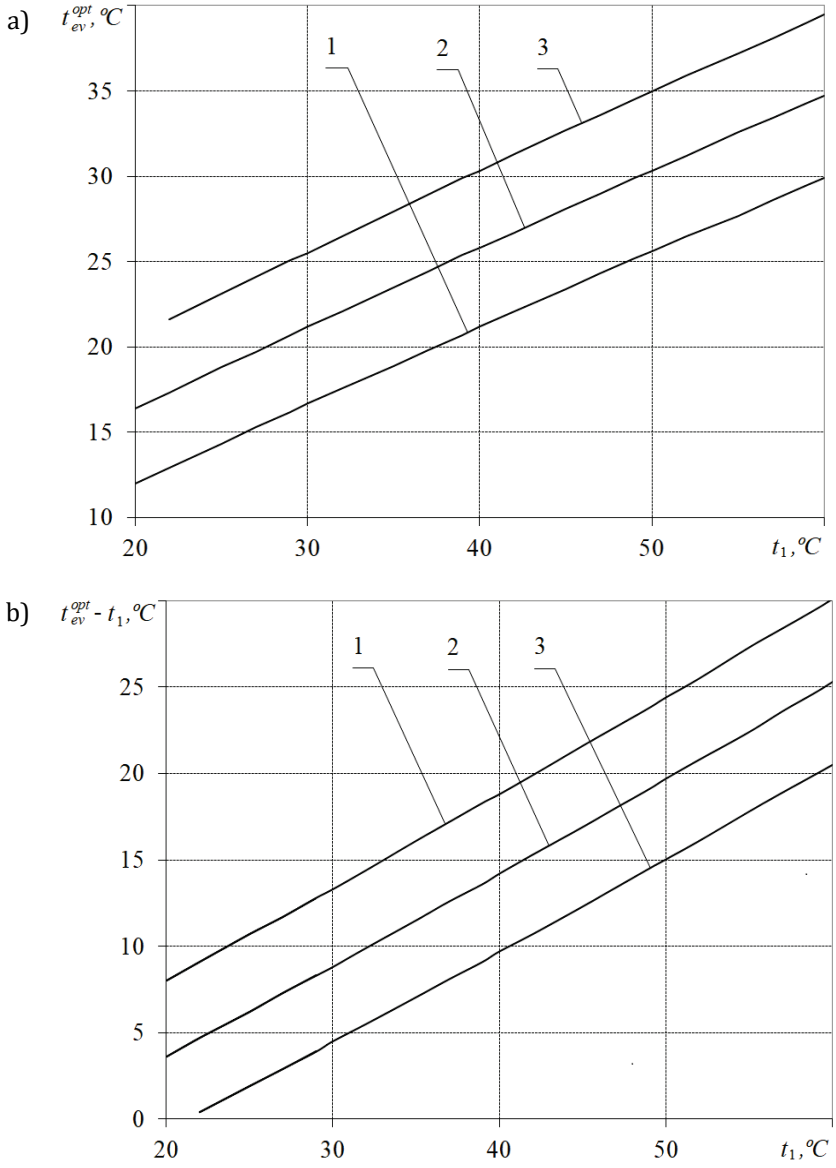

FIGURE 3. *Dependence of: a) the optimum temperature of the technogenic air source at the outlet of the HP evaporator from the temperature of technogenic air emissions, b) the degree of use of technogenic air source from the temperature of technogenic air emissions, respectively 1-3 – design temperature of heating coolant in the heating system* t_c^{est} *= 40 °C; 50 °C; 60 °C*

By further numerical analysis, it was found that with changes in ambient temperature, the values of the optimal temperatures of the technogenic air source at the outlet of the HP evaporator, and the corresponding maximum beneficial effects, also change. The results of this analysis for the optimal air temperature at the outlet of the HP evaporator are presented in Figure 4.

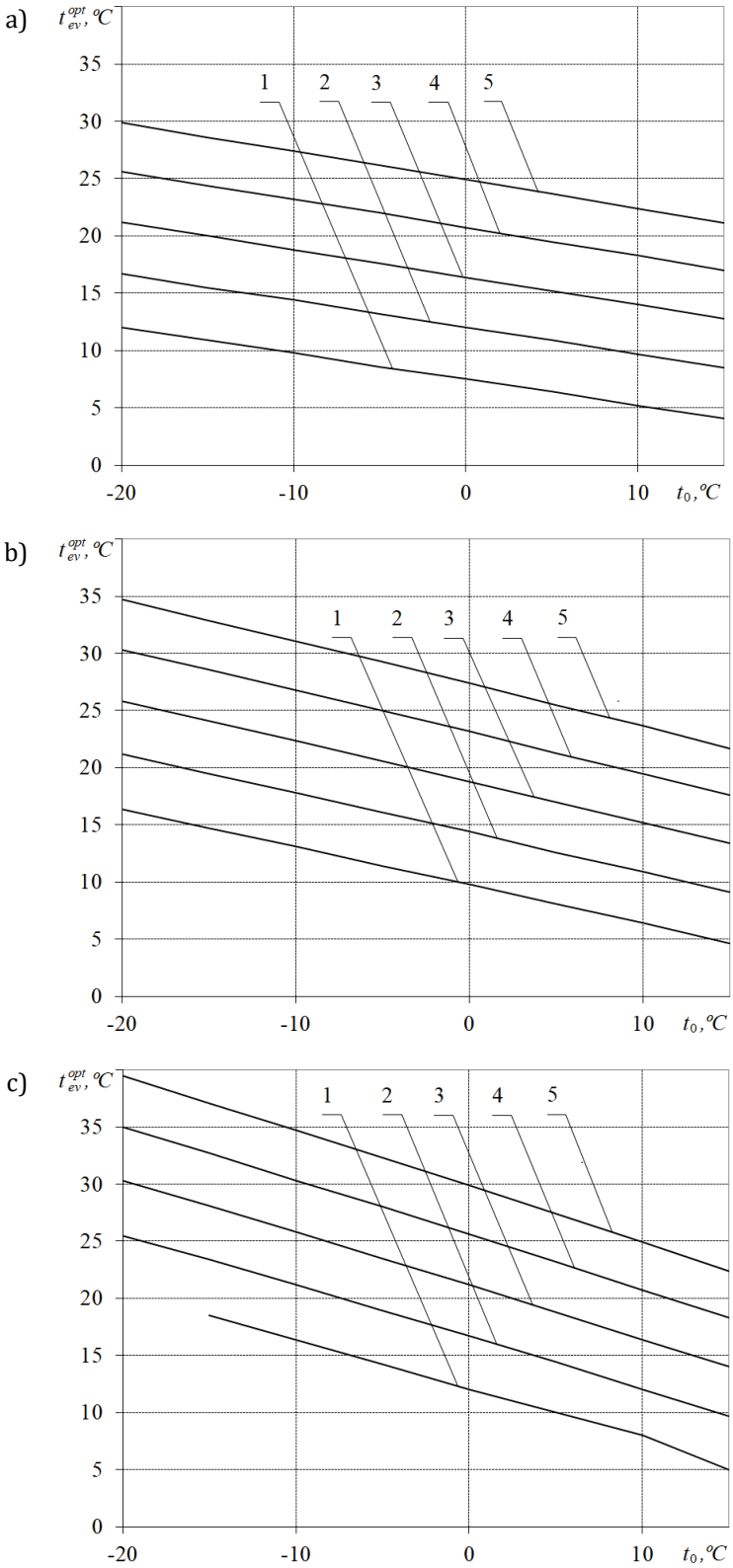

FIGURE 4. *Dependence of the optimum temperature of the technogenic air source at the outlet of the HP evaporator on the outside air temperature: a), b), c) the calculated temperature of the heating coolant in the heating system t_c^{est} = 40 °C; 50 °C; 60 °C, respectively 1-5 – at the temperature of technogenic air emissions t_1 = 20 °C; 30 °C; 40 °C; 50 °C; 60 °C*

Based on these dependences, the dependences of the optimal degree of heat utilization of air emissions (optimal temperature difference $t_1 - t_{ev}^{\text{opt}} = \Delta t_{ev}^{\text{opt}}$) were obtained, which are presented in Figure 5.

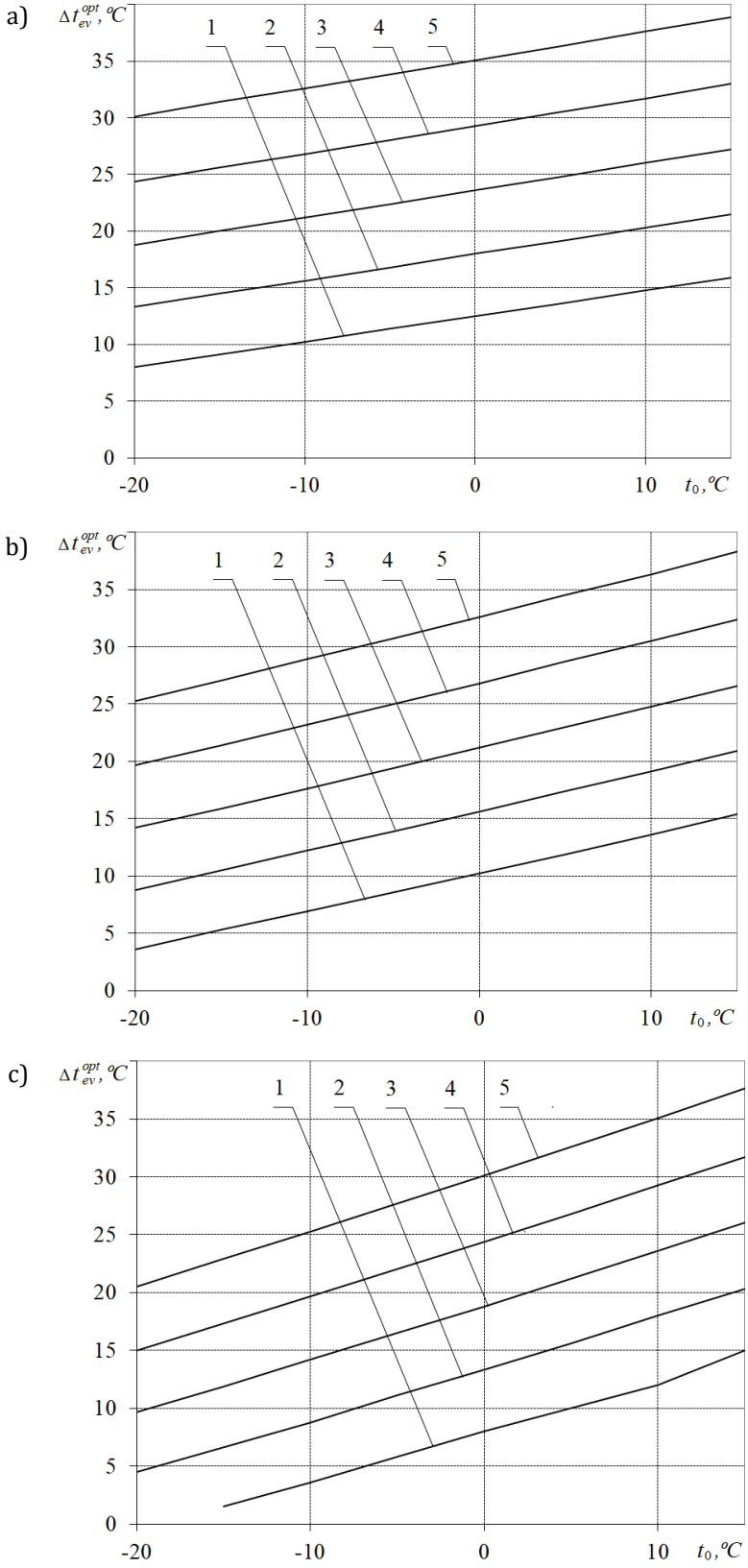

FIGURE 5. *Dependence of the degree of use of technogenic air source on the outside air temperature: a), b), c) the calculated temperature of the heating coolant in the heating system t_c^{est} = 40 °C; 50 °C; 60 °C, respectively 1-5 – at the temperature of technogenic air emissions t_1 = 20 °C; 30 °C; 40 °C; 50 °C; 60 °C*

The graphs show that the decrease in ambient temperature for all other parameters of the system (t_1 and t_c^{est}) leads to a decrease in the optimal temperature difference Δt_{opt} which corresponds to the maximum of useful effect as at the same time working conditions of the heat pump owing to the increase in temperature of the heat carrier worsen in heating system. It should be noted that with lowering the temperature of ventilation emissions below t_1 = 20°C for heat pump heating system with a design temperature t_c^{est} = 60°C at ambient temperature t_0 = –20°C the value of the optimal temperature difference Δt_{opt} decreases to negative values, which means no useful effect from utilization of air emissions and for their further utilization in the heating system an additional lower heat source is required with additional consumption of external energy to increase its potential.

To compare the energy efficiency of heat pump heating systems using the heat of technogenic air emissions and the heat of atmospheric air, specific costs of external energy for the heat pump heating system on the ambient temperature are plotted. The corresponding dependences are presented in Figure 6.

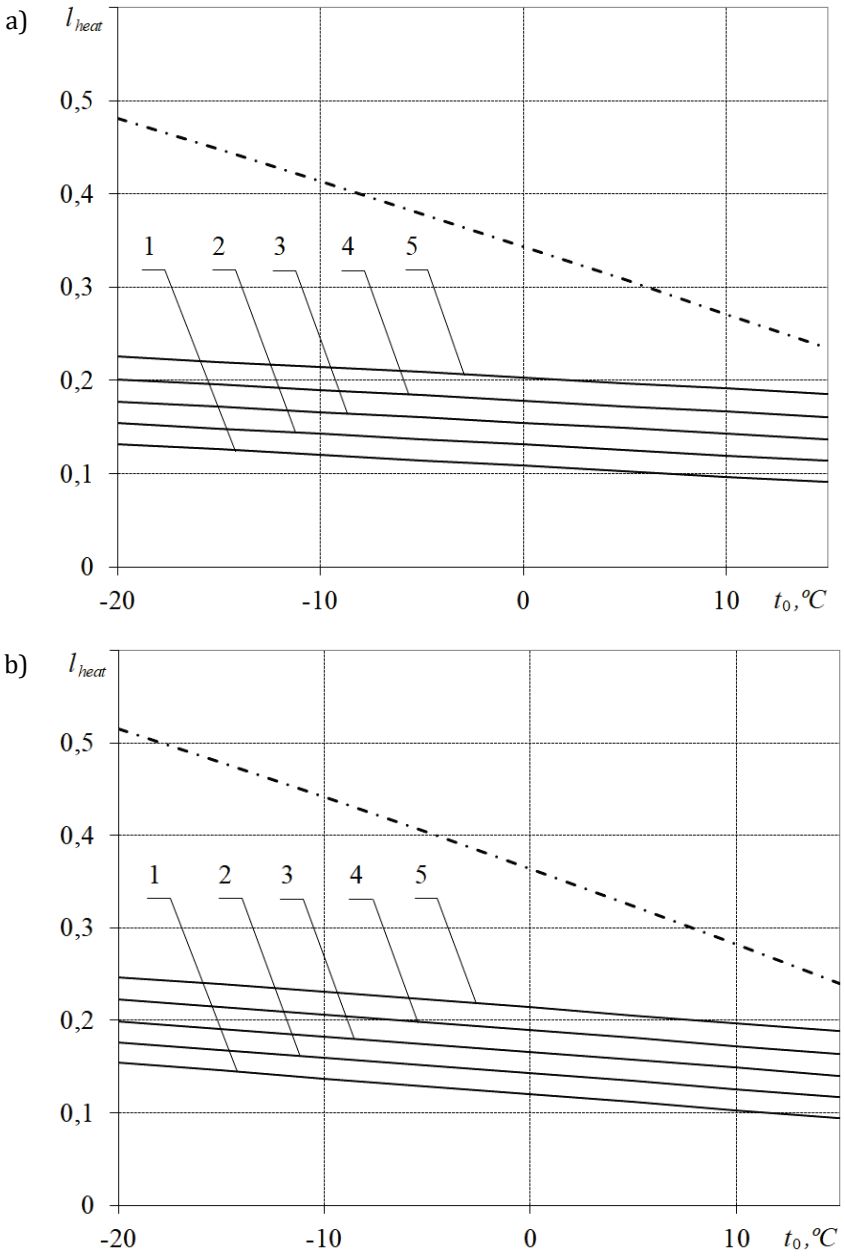

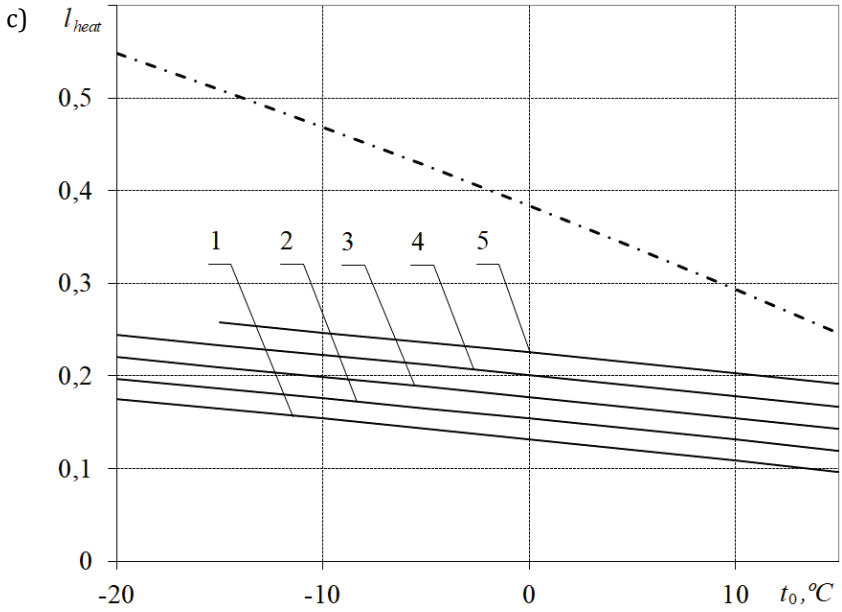

FIGURE 6. *Dependence of specific costs of external energy for the heat pump heating system on the ambient temperature: a), b), c) the calculated temperature of the heating coolant in the heating system* t_c^{est} *= 40°C; 50°C; 60°C, respectively: 1-5 – at the temperature of technogenic air emissions* t_1 *= 20°C; 30°C; 40°C; 50°C; 60°C*

As it can be seen from the graphs, the use of heat from techogenic air emissions is characterized by much lower specific energy consumption. The energy effect increases with decreasing ambient temperature due to the independence of the lower source temperature from the ambient temperature.

Conclusions

Analysis of the results of the study presented in this section allows us to draw the following conclusions.

1. The use of heat of technogenic air emissions in low–temperature heat pump heating systems allows to obtain a useful energy effect in the form of the difference between the utilized heat and the heat consumption of the primary fuel to drive the heat pump.
2. The maximum value of the beneficial effect is achieved under conditions of optimal use of heat of air emissions in the heat pump, ie under conditions of achieving the optimal value of the temperature difference between the inlet and outlet of the heat pump evaporator.
3. The optimal degree of heat use of air emissions in the heat pump (and, accordingly, the beneficial effect) increases with increasing temperature of technogenic emissions and with decreasing design temperature of the heating coolant in the heating system and decreases with decreasing ambient temperature.
4. When the emission temperature is reduced below 20°C and the outside air temperature to –20°C, the useful energy effect of air emissions disappears, ie to provide a heating system there is a need to use an additional lower heat source with additional external energy consumption for the heat pump.
5. The specific costs of external energy in the heat pump system using technogenic air emissions are weakly dependent on the ambient temperature and at its design temperature t_0 = –20°C can be reduced compared to the system using the heat of ambient air by about 3 times.

Conflicts of Interest: The author declares no conflict of interest.

References

[1] European Heat Pump Association (EHPA) [Electronic resource]. Access mode – http://www.ehpa.org/.

[2] Bezrodny M.K., Prytula N.O., *Thermodynamic and energy efficiency of heat pump schemes of heat supply:* Monograph. K.: NTUU "KPI" Publishing House "Polytechnic", 2016, 272p.

[3] Tkachenko O.O., *High–temperature processes and installations*: Textbook. K.: A.C.K., 2005, 480 p.

[4] Zhang J., Wang R.Z., Wu J.Y., *System optimization and experimental research on air source heat pump water heater*. Applied Thermal Engineering 27 (5, 6) (2007), pp. 1029-1035.

Tetyana NIKULENKOVA[1]

Anatolii NIKULENKOV[2]

[1] *National Technical University of Ukraine "Igor Sikorsky Kyiv Polytechnic Institute", Kyiv, Ukraine*

[2] *Separated Subdivision «Scientific and Technical Center» of the State Enterprise «National Nuclear Energy Generating Company «Energoatom», Kyiv, Ukraine*

Corresponding author: Tetyana.nikulenkova@gmail.com

DOI: 10.53412/jntes-2021-1.4

FEATURES OF RESIDUAL SERVICE LIFE DETERMINATION FOR HIGH PRESSURE ROTORS OF K-200-130 AND K-1000-60/3000 TURBINES

Abstract: *So far, certain approaches have been developed to extension of service life of equipment in the different stages of metal physical exhaustion. The possibility of defining operating conditions of plant equipment beyond the fleet service life becomes even more relevant with increased operating time. The service life is determined as an individual one and is assigned based on the results of individual an inspection of a separate element or the largest group of single-type equipment elements of the considered plant. The fleet service life being reached is followed by diagnostics of specific units of power installations and analysis of their operation, measurement of actual dimensions of components, examination of structure, properties and damage accumulation in the metal, non-destructive testing and estimate of stress strain state and residual service life of the component. The results of performed studies are used to determine an individual service life of each element of energy equipment.*

Keywords: *service life, steam turbine, temperature, boundary conditions, ANSYS, 2-D and 3-D geometrical models, K-200-130, K-1000-60/3000, nuclear power plants*

Introduction

The present situation in the energy market of Ukraine demonstrates the need to increase operating capacities, thus requiring renovation or complete replacement of equipment of thermal power plants during the next years. This would allow lifetime extension of thermal power units, including expanding installed capacity and load-following range, as well as decreasing the specific fuel consumption per kWh production.

The problem of defining service life of nuclear power plants considering life cycles of their major equipment is becoming increasingly important each year. This raises questions relating to reasonable decision-making scheme on the due time for decommissioning of NPPs and feasibility of replacing of any major equipment considering safety and economic factors.

Purpose and research objectives

The purpose of the paper is to justify a comprehensive scheme to assessment of residual service life of steam turbine rotors and extension of the operating life [1].

The set purpose is to be achieved by reaching the objectives as follows:

1. Analysis of the known ways for service life extension of energy equipment that has reached the end of its fleet service life.
2. The results of metal inspection throughout the entire operating lifetime and analysis of technical audit data relating to damages and geometry changes during refurbishment of steam turbine elements.
3. Analysis of the results of experimental researches and estimate of residual service life of steam turbines considering actual operating conditions and local damages of separate turbine components.
4. Elaborating proposals regarding approaches to extension of service life of steam turbines.

Material and research results

Initial data. The condensate steam turbines of thermal and nuclear power plants with high temperature elements in 3-D setting are considered. The boundary conditions are established for heat exchange on the rotor surfaces using ANSYS digital model based on built geometrical 3-D models corresponding to operating modes by start-up types from cold, hot and warm conditions and stationary mode.

Model description. In the first phase of the calculation a method for building spatial analogues of turbine machine elements was developed using Solidworks for high and medium pressure rotors.

In the second phase a method for solving non-stationary thermal conductivity equation was developed and boundary conditions of heat exchange on the surfaces of rotors were established using the ANSYS digital model based on 2-D and 3-D geometrical models. The boundary conditions (BC) correspond to operating modes by start-up types from cold, hot and warm conditions, stationary regime [2].

The problem of non-stationary thermal conductivity of steam turbine elements is solved with the equation type as follows:

$$div(\lambda gradt) = c\gamma \frac{\partial t}{\partial \tau} \tag{1}$$

where λ, c, γ are temperature functions and coordinates under the initial conditions $t_0 = t(x,y,z,0) = f_0(x,y,z)$ and the boundary conditions of the I, II, III or IV kind.

The non-stationary boundary conditions of the I-IV kind were set with due account of operating transients for the surfaces of spatial geometrical models of LPC and IPC.

When defining the BC for non-stationary operating modes the estimate of steam temperature in transient modes on the surfaces of steam turbine elements was applied. Under rapid changes of operating mode of the turbine one can observe a fast change of steam temperatures in its flow section. It has been established by experimental means that in the initial phases of power unit start-up the temperatures of main and reheat steam measured by regular sensors are lower than real temperature values of the steam both by their change speed and statically. Therefore, it was suggested to use the following method for estimation of temperature under transient modes of steam turbine (based on example of calculation of steam temperature in the control stage chamber that almost coincides with the temperate after the control stage).

The third phase implies application of the ANSYS digital model to determine the stress strain state of the HPC and IPC rotors with account of their complex spatial geometry, damages during operating period, repair and restore modifications of design geometry. The temperature gradient is used as a criterion to determine stresses when analyzing their behavior in the high temperature elements of steam turbine for operating modes. The distribution of stress strain state was calculated for the moments when temperature gradients reached extreme values.

The stress strain state was determined for:

- pressure loads;
- temperature loads;
- loads of centered forces (ω = 3000 rpm);
- loads of gravity forces;
- reaction resistance.

The calculations included defining principal stresses, stress intensity for the entire period corresponding to start-up and stationary operating modes in all division points of the high temperature elements of the steam turbine.

That start-ups of the turbine from different thermal conditions can be accompanied with thermal stresses on the rotor surface, which increase the yielding limit leading to residual strain of the metal. If physical and mechanical properties are come out in different values of the yielding limit σ along the cross section area of the shaft, then after reaching σ multiple times a summing of residual axial strains appears, and this is one of the causes of rotor bow.

In the fourth phase a methodological approach was developed to calculate the low cycle fatigue using a software complex of NTUU KPI and ANSYS digital models with application of the calculated change of the stress strain state of HPC and IPC shells and rotors and with account of optimized strength margin ratios by the number of cycles and deformations [3].

Analysis of the study results. The capability of forecasting the value of the residual life is provided under the conditions as follows:

- parameters defining technical condition of equipment are known;
- criteria of the boundary state of the equipment are known;
- it is possible to perform periodical or continued inspection of the technical state parameters.

The remaining operating life before cracks $[G]_{oct}$ (in years) is determined with the formula:

$$[G]_{oct} = \frac{1-\Pi'}{\Pi''_g} \tag{2}$$

where:

Π' – total damage accumulated in the metal of rotos and shells operating under combined creep implication in the different modes of q' types and cycle loading under different transient modes of k' types;

Π''_g – the forecasting average annual loading for the operating period following the analysis that will be accumulated in the considered area of the rotor and shell during the alternation of q'' types of sustainable mode and k'' types of cycle.

All values relating to the period of operation after carrying out an estimation and continuation of a resource are marked by two strokes.

The author proposes to determine a total damage Π' accumulated in the metal of the rotors operating in conditions of joint action of creep at different steady modes and cyclic loads at different variable modes, by an improved formula, considering [4] and the effect of torsional vibrations:

$$\Pi' = \Pi'_{st} + \Pi'_c + \Pi'_{kp.k} = \sum_{j=1}^{q'} \frac{t'_j}{T'_{pj}} + \sum_{l=1}^{k'} \frac{n'_l}{N'_{pl}} + \sum_{i=1}^{s'} \frac{r'_i}{R'_{pi}} \tag{3}$$

where:

$\Pi'_{st}, \Pi'_c, \Pi'_{kp.k}$ – static, cyclic damage and damage from torsional vibrations accumulated in the area of the rotor checked at the time of assessment of the extension of service life;

$t_j^{'}$ – operating time in the j steady mode under the temperature of metal $T_{pj}^{'}$ and equivalent local creep stresses $(\sigma_{aj}^{'})_{\max}$;

$T_{pj}^{'}$ – time before the boundary state is reached subject to equivalent stresses $(\sigma_{aj}^{'})_{\max}$ under temperatures $T_j^{'}$ according to the diagram of long-standing strength of material;

j – number of different types of steady modes at the time of assessment with temperature $T_j^{'}$ and steady equivalent local creep stresses $(\sigma_{aj}^{'})_{\max}$;

$n_l^{'}$ – number of cycles of i type;

$N_{pl}^{'}$ – number of cycles before fatigue cracks appear only subject to cyclic loadings of i type;

k' – number of different cycle type at the time of assessment with different ranges of specified stresses $\Delta\sigma_l^{'}$ and strain amplitudes $\varepsilon_l^{'}$;

$r_i^{'}$ – number of loading cycles with strain amplitude τ_{ai} (τ_{ai} – amplitude of i cycle of the damped process);

$R_{pi}^{'}$ – number of cycles before damage under cyclic loading with strain amplitude $(\tau_{ai})_{\max}$ from torsional vibrations;

s' – number of stress levels (units).

All values relating to analysis of the previous operating period are marked by a stroke.

The forecasted residual service life of the high temperature equipment of steam turbine was determined with the formula:

$$[T]_{oct} = \frac{1}{\Pi'} \tag{4}$$

where Π' – summed damage.

When determining the reliability of equipment, the probabilistic methods of life estimation are changed for estimation of the individual life of aging equipment based on an integrated approach that combines destructive and non-destructive inspections supported by verifying calculations of strength [5-7]. There has been a tendency in the life estimation to switch from flaw detection to technical diagnostics methods raising the need in comprehensive examination of aging equipment in order to identify potentially dangerous zones.

There is no established procedure for comprehensive application of different techniques and means of non-destructive and destruction inspections to a specific item under inspection. The sequence, procedure, scope and frequency for inspection of a component are determined by fleet (estimated) life, damage, overhaul period, as well as the availability of means and techniques for metal inspection of equipment.

Extending the service life of existing power units is a common international practice with an important task to keep producing electricity at the achieved level until deployment of new capacities at thermal power plants.

A unique feature of the modern energy sector is operation of a significant number of turbines with expired intended service life. At the same time, domestic and foreign practice shows that the actual service life of turbines often significantly exceeds the term specified by the manufacturer.

A comprehensive study flow diagram for life extension of K-200-130 and K-1000-60/3000 turbine rotors with expired fleet life was improved within this scientific paper based on the technical audit of energy equipment of steam turbines using examinations of low and creep fatigue, and long term strength of rotors, as well as assessment of shaft line damages due to torsional vibrations. The main principal decisions within the comprehensive flow diagram for estimation of the residual life of large-scale steam turbine rotors is provided in Figure 1.

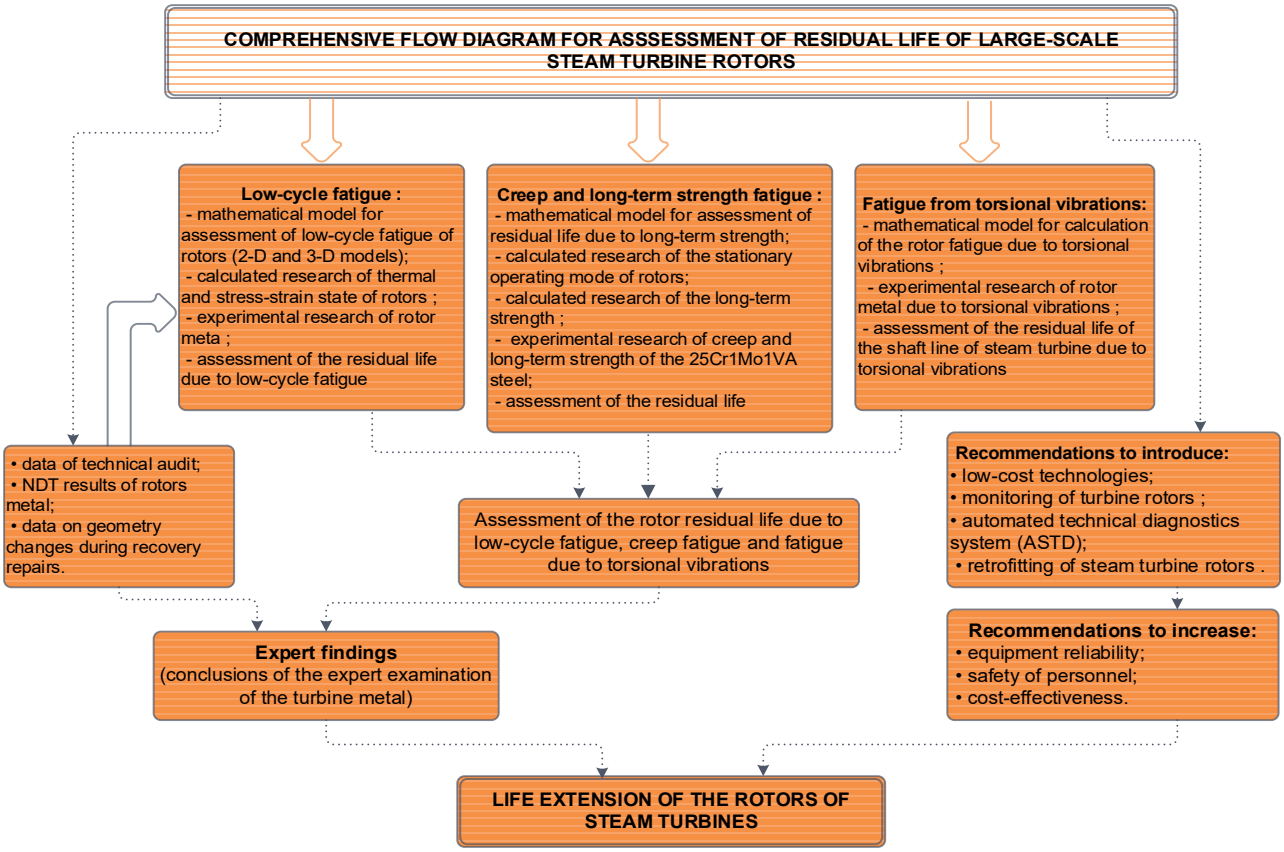

FIGURE 1. *Comprehensive flow diagram for assessment of the residual life of the steam turbine rotors*

The main reason for consideration of long-term operation of power plant equipment is that the cost of extending the service life of high-temperature equipment is several times less than buying new ones. Under such circumstances, one of the most important diagnostic tasks, formally not provided by regulations, is the assessment of residual life. This problem is not simple and cannot be solved by conducting standard studies.

The first element for estimating residual life of steam turbine rotors is low cycle fatigue of K-200-130 and K-1000-60/3000 turbine rotors. Based on the results of the technical audit and visual inspection conclusions, different types of damage are localized in the geometric model of the element in the form of metal samples of different shapes. The estimated temperatures at individual points of the metal of the high and intermediate pressure cylinder rotors were determined for their further use in calculating the number of cycles before failure. This approach allowed to bring the calculated model of steam turbine rotors closer to the real state after long-term operation [8, 9]. Calculated studies of thermal, stress-strain state and low-cycle fatigue of rotors allowed to develop recommendations of constructive and mode nature, which reduce temperature stresses in start-up modes and metal damage accumulation.

The second element for estimating residual life of steam turbine rotors is a calculated and experimental study of long-term strength. The calculated studies of TC and SSS of the rotors of K-200-130 and K-1000-60/3000 steam turbines in the stationary mode of operation were performed, creep stresses and strains were determined and the data on residual life was received [10, 11].

The third element for estimating residual life of steam turbine rotor is fatigue from torsional vibrations. The mechanism of torsional vibrations of shafts is one of the main causes of metal cracking of turbine rotors and their fracture, often with catastrophic consequences.

Conclusion

The main reason for consideration of long-term operation of power plant equipment is that the cost of extending the service life of high-temperature equipment is several times less than buying new ones.

Under such circumstances, one of the most important diagnostic tasks, formally not provided by regulations, is the assessment of residual life. This problem is not simple and cannot be solved by conducting standard studies.

When forecasting, depending on the service life of the equipment, two approaches are used. Fort short service life (relatively to fleet) and insignificant damage of the equipment only the information on loading is used for forecasting of its residual life. With a service life close to the fleet or significant damage to the equipment elements the degree of equipment damage is additionally investigated. The advantage of the first approach is its lower complexity, the second, which we adhere to – is a more accurate forecast allowing to identify additional reserves of equipment life.

Conflicts of Interest: The author declares no conflict of interest.

References

[1] Peshko V., Chernousenko O., Nikulenkova T., & Nikulenkov A., *Comprehensive rotor service life study for high & intermediate pressure cylinders of high power steam turbines*, Propulsion and Power Research, 2016, vol. 5(4), pp. 302-309. doi: 10.1016/j.jppr.2016.11.008.

[2] Chernousenko O., Nikulenkov A., Nikulenkova T., Butovskiy L., & Bednarska I., *Calculating boundary conditions to determine the heat state of high pressure rotor of the turbine NPP K-1000-60/3000*, Bulletin of the National Technical University "KhPI", 2018, vol. 12(1288), pp. 51-56. doi: 10.20998/2078-774X.2019.03.01.

[3] Nikulenkova T., Nikulenkov A*., Calculation of boundary conditions using CFD modeling as part of a comprehensive approach to impact assessment of modifications on the service life of critical elements of a nuclear power plant turbine*. The 16th International Conference of Young Scientists on Energy Issues, 2019, VII, 267-278.

[4] Wähner H., *Turbinenleitrechner TENSOSIM auf microprozessorbasis zur Thermischen Überwachung von Dampftuhinen*, Wähner H., Preusse W., Tappe W. u.a., Mitteilungen Kraftwerksanlagenbau DDR. 1984. Bd. 1. No. 12, S. 16-20.

[5] RTM 108.020.16-83. Calculating the Temperature Fields of Steam Turbine Rotors and Housings, M., 1985, 115p.

[6] RTM108.021.103, Details of stationary steam turbines. Low cycle fatigue calculation. M., 1985. No. AZ-002/7382, 49 p.

[7] RD34.17.440-96, Methodological guidelines to perform works within assessment of individual service life of steam turbines and its extension beyond the fleet service life. M., 1996, 47p.

[8] Chernousenko O., Rindyuk D., & Peshko V., *The strain-stress state of K-1000-60/3000 turbine rotor for typical operating modes*, Bulletin of the National Technical University "KhPI", 2019, vol. 3(1328), pp. 4-10. doi: 10.20998/2078-774X.2019.03.01.

[9] Chernousenko O., Rindyuk D., & Peshko V., *Features of prolongation of the service life of high- and intermediate-pressure rotors of K-200-130 steam turbine of Luhansk TPP*, The Problems of General Energy, 2018, vol. 2(53), pp. 65-70. doi: 10.15407/pge2018.02.065.

[10] Nikulenkov A., Samoilenko D., and Nikulenkova T., *Study of the impact of NPP rated thermal power uprate on process behavior at different transient conditions*, Nuclear and Radiation Safety, 2018. vol. 4(80), pp. 9-13. doi: 10.32918/nrs.2018.4(80).02.

[11] Chernousenko O., & Peshko V., *Assessment of Resource Parameters of the Extended Operation High-Pressure Rotor of the K-1000-60/3000 Turbine*, Journal of Mechanical Engineering, 2019, vol. 4(22), pp. 41-47. doi: 10.15407/pmach2019.04.041.

Iuliia KUIEVDA
Serhii BALIUTA
Petro ZINKEVICH
Oleksandr STOLIAROV
National University of Food Technologies, 68 Volodymyrska str., 01601 Kyiv, Ukraine
Corresponding author: e-mail: julika@gmail.com

DOI: 10.53412/jntes-2021-1.5

FORECASTING THE ELECTRICITY GENERATION OF PHOTOVOLTAIC PLANTS

Abstract: *Due to the need in accordance with Ukrainian legislation to submit a day-ahead hourly forecast of electricity generation of solar power plants, the problem of forecasting model quality becomes very important. In the study it is proposed a method of choosing the optimal structure and sensitivity assessment of ANFIS-based forecasting model. In the model the input is solar irradiance, the output is solar panel generation power. The method is based on computational procedures using MATLAB software. For the data set, used in the study, the results, optimal for normalized mean absolute error (NMAE), were achieved on 5 triangular input member functions (trimf), while the error varied within 0.23% depending on number and shape of input member functions. According to the calculations of input error sensitivity of the forecasting model with 5 input trimf membership functions, the increasing of input error up to 8.19% NMAE leads to the raising of the output error in the testing sample up to 5.78%, NMAE. The rather low sensitivity of the model to the input data error allows us to conclude that forecasted meteorological data with a pre-known fixed forecast error can be used as input data.*

Keywords: *solar power plants; forecasting; ANFIS; fuzzy inference system.*

Introduction

Since 2019, the electricity market in Ukraine has moved to a new model of operation. Producers from Renewable energy sources (RES) make up an increasing share of the market. According to Ukrenergo [2], in March 2021 the installed capacity of RES in Ukraine was 6.97 GW, of which the largest share falls on solar power plants (SPP) – 5.51 GW, namely 10% of the total installed generation capacity in the country. RES producers sell electricity at a "green tariff", which is the highest among all others in Ukraine. From the beginning of 2021, RES producers began to compensate for the imbalance of electricity in the market a day in advance relative to the day-ahead hourly generation forecast that they provide before the start of the market day.

All these circumstances have increased the importance of the tasks of forecasting the generation of electricity from RES producers, in particular SPP, both at the level of the power system of Ukraine as a whole and at the level of producers.

The day-ahead hourly forecast of SPP generation is referred to as short-term forecasts and it is used physical, statistical, and intelligent methods [1]. Among the intelligent forecasting methods, the most popular are models based on the Artificial Neural Networks (ANN) and Adaptive Neuro-Fuzzy Inference Systems (ANFIS), as well as combinations thereof. For example, in [5] and [6] new combined methods are presented, which include ANN and ANFIS for short-term forecasting of SPP generation.

The above publications describe the classical and new methods of forecasting and include assessment of their accuracy, but it is paid not enough attention to the study of the properties of the models themselves, in particular their structure and sensitivity to input error. The latter is especially true for models that use intelligent technologies, such as ANN and ANFIS, where it is impossible to explicitly express the relationship between input and output variables.

The aim of this work is to form an approach to the study of the forecast error dependence on the number of input membership functions and their form, as well as the sensitivity to input data error of the ANFIS-based day-ahead hourly forecast SPP generation model. The sensitivity of the model to input data error is particularly important because the input data for generation forecasting can come from meteorological forecast providers, which indicate the predefined forecast error.

Materials and Methods

In the study it was built a numerical model of the dependence of solar panel generation power on current solar irradiance based on ANFIS 3. This model can be used for hourly day-ahead generation forecast based on solar irradiance forecast values from weather forecast providers, considering the cloud opacity.

The ANFIS methodology is based on a network of special structure that allows to create and configure a set of fuzzy rules such as Takagi-Sugeno to approximate the relationship between multiple inputs and a single output. The author of ANFIS in [3] showed that it is a universal approximator of continuous functions of several variables defined on compact sets.

Data from the open dataset Photovoltaic (PV) Solar Panel Energy Generation from UK Power Networks from the London Datastore repository were used to train and test the model [4]. The input data of the model – current solar radiation (W/m^2), measured at the local weather station, and the output data – the power of the solar panel (kW) from the location of Forest Road. For the research, the sample was divided into training and testing data. In Figure 1 it is given the graph of input and output data and shown training sample in blue, while testing sample in red.

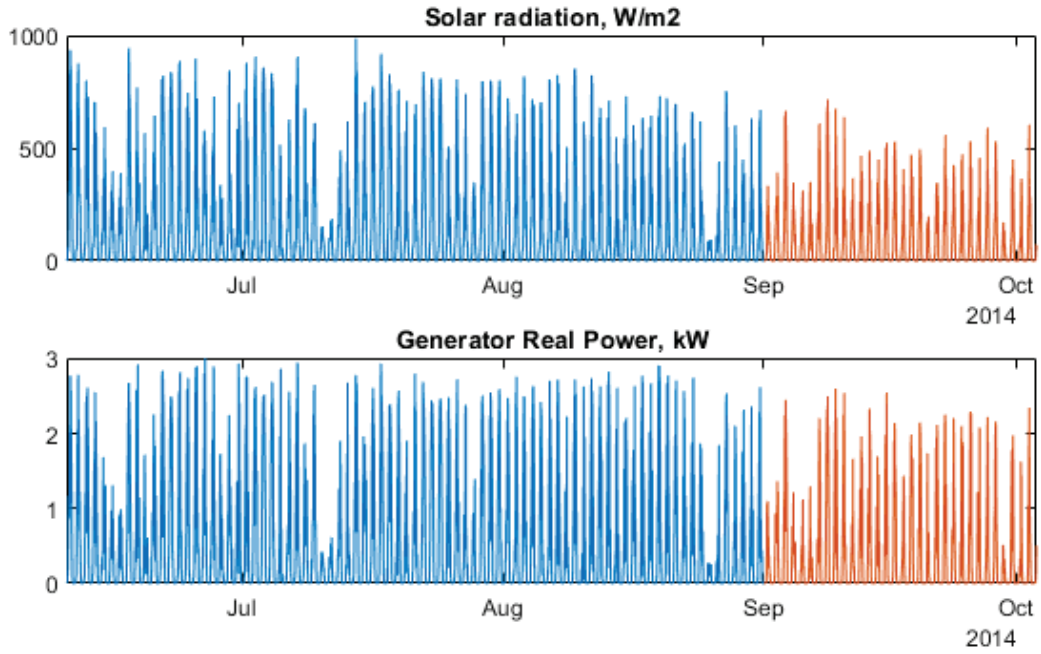

Figure 1. *Data from the location of Forest Road (open dataset Photovoltaic (PV) Solar Panel Energy Generation), training sample is blue, testing sample is red*

The research was performed using numerical simulation in MATLAB with the use of Fuzzy Logic Toolbox. The first part of the research was devoted to the choice of the number of input membership

functions and their form. In the second part of the study, the sensitivity of the model to the input data error was determined for the selected number and form of membership functions from the first part. The results were evaluated by errors root mean square error (RMSE), mean absolute error (MAE) and normalized mean absolute error (NMAE):

$$\mathrm{RMSE} = \sqrt{\frac{1}{N}\sum_{i=1}^{N}\left(\hat{y}_i - y_i\right)^2} \tag{1}$$

$$\mathrm{MAE} = \frac{1}{N}\sum_{i=1}^{N}\left|\hat{y}_i - y_i\right| \tag{2}$$

$$\mathrm{NMAE} = \frac{100}{N}\sum_{i=1}^{N}\frac{\left|\hat{y}_i - y_i\right|}{y_{\max}} \tag{3}$$

where:

y_i – are observation values;

$\hat{y}_i$ – predicted values;

$y_{\max}$ – maximum value of the observed variable.

Results and Discussions

It was calculated the table of dependence of RMSE, MAE and NMAE errors on the number of input membership functions and their forms for training, testing and the whole sample. The number of input membership functions varied from 2 to 30, and the type of membership functions (MF) was chosen from the set (MATLAB notation [7]): Generalized bell-shaped MF (gbellmf), Gaussian MF (gaussmf), Gaussian combination MF (gauss2mf), Triangular MF (trimf), Trapezoidal MF (trapmf), Difference between two sigmoidal MF (dsigmf), Product of two sigmoidal MF (psigmf), Pi-shaped MF (pimf).

To determine the optimal number and form of input membership functions, the NMAE error of the testing sample was used. Figure 2 shows graph of NMAE errors which were calculated from identified on training sample ANFIS models with 8 types of input membership functions from the set, mentioned above. Each line in the graph corresponds to specific type of membership function, *x*-axis shows the number of membership functions.

As can be seen in Figure 2, NMAE varies in the range from 3.92% to 4.15%, and minimum is achieved on 5 triangular trimf membership functions (4) with tunable parameters *a*, *b*, *c,* which shapes are shown in Figure 3. Let us call this model ANFIS5trimf.

$$f(x) = \max\left(\min\left(\frac{x-a}{b-a}, \frac{c-x}{c-b}\right), 0\right) \tag{4}$$

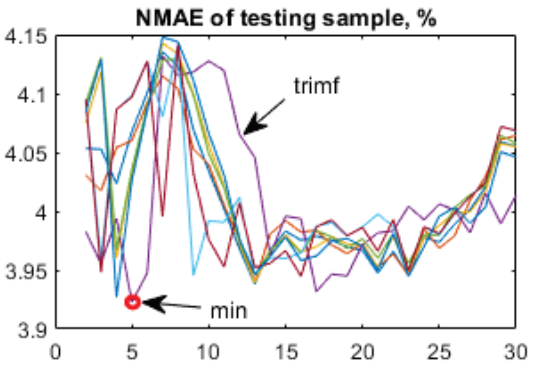

Figure 2. *Minimum of NMAE on testing sample*

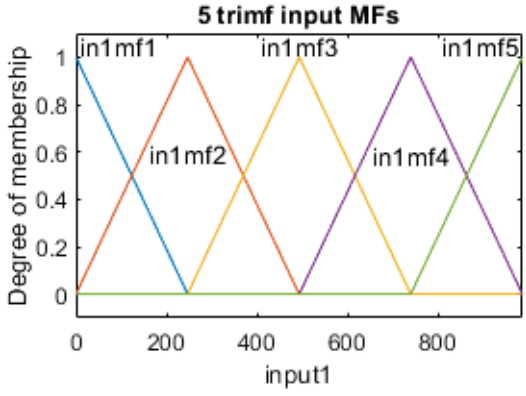

Figure 3. *5 input triangular membership functions*

The structure of ANFIS5trimf is presented in Figure 4. As shown in the figure, the model consists of 1 input – solar radiation in (W/m²), 1 output – power of the solar panel (kW), 3 layers of 5 nodes, which represent trimf input, linear output membership functions and fuzzy logical operations, and 1 summarizing layer to produce the output value.

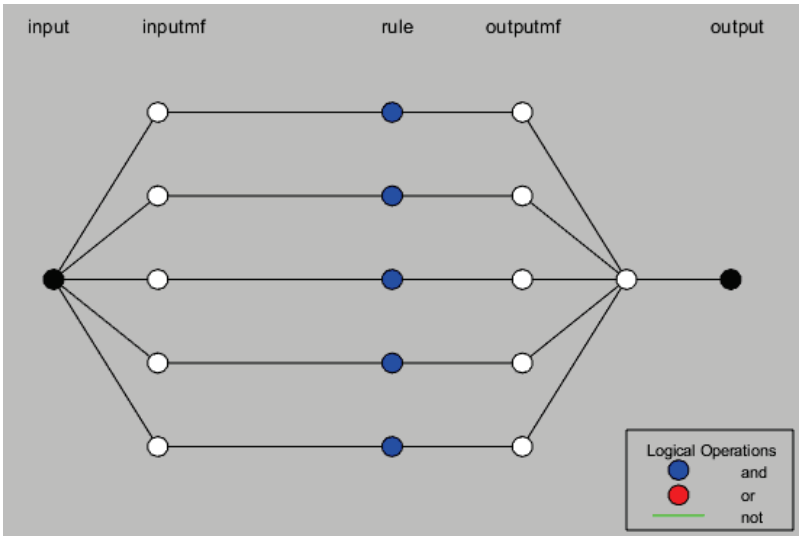

FIGURE 4. *The structure of ANFIS model with 5 input membership functions*

Figure 5 demonstrates scatterplot of dependence of solar panel generation power on measured solar irradiance from the Forest Road data set, mentioned above. The training sample consists of blue dots, and testing sample – of orange dots. The red curve stands for the output surface of trained ANFIS5trimf, while the green curve shows the result of linear regression. For comparison of ANFIS5trimf and linear regression models on the testing sample it was calculated RMSE (1): 0.2444 and 0.2641 correspondingly, which means that ANFIS5trimf better fits the data than linear regression.

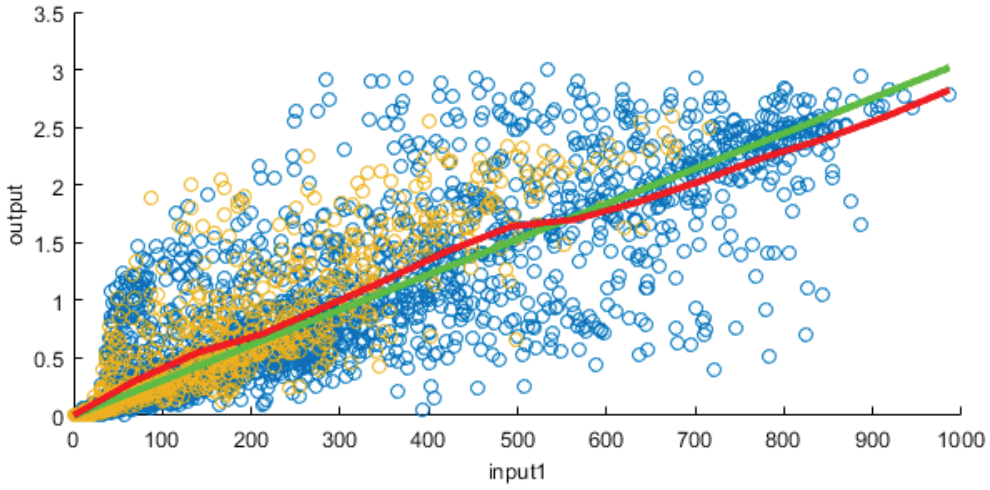

FIGURE 5. *Solar radiation in training (blue) and testing (orange) samples with ANFIS5trimf output surface (red) and linear regression curve (green)*

As can be seen in Figure 5 the data are rather widely spread out from the approximating curves. There are some possible reasons of that, which can be considered for both variables in data set. For measurements of solar radiation by solar sensor at the local weather station it can be mentioned that they are taken from close but different place than solar panels location, solar panels can take large area and be under different cloud conditions, furthermore the dirt and snow can influence its

measurements. For generator power data there are also some additional influencing factors, such as uneven shading, precipitation, level of degrading of PV modules, and their availability, etc. All these factors can be considered to make the model more accurate for further researches.

Figure 6 shows the example of ANFIS5trimf forecast for one week of testing sample: purple line consists of forecasted values, and orange line consists of measured values.

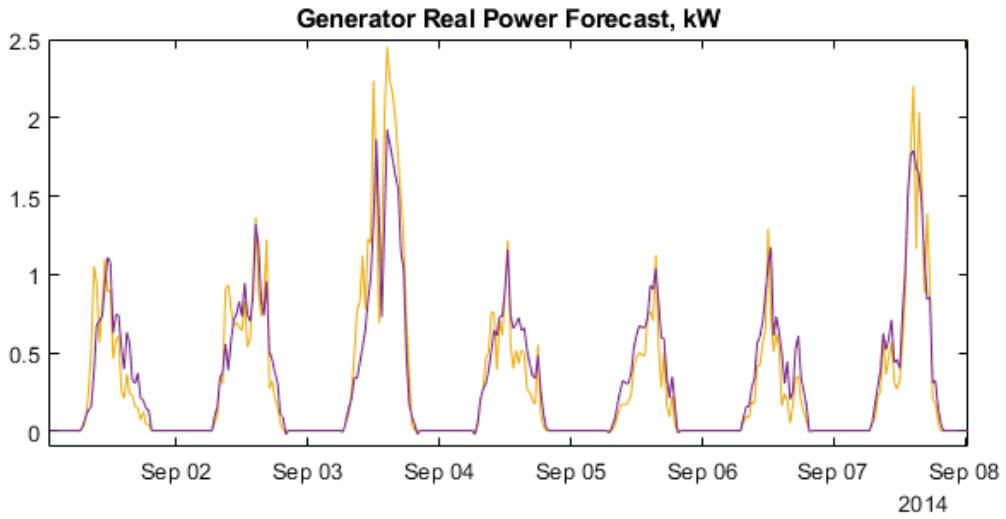

FIGURE 6. *ANFIS forecast of generator real power, where forecasted values are purple and measured values are orange*

The ANFIS5trimf model was tested for sensitivity to the error of the input data. The generated random sequences with different variances were sequentially added to the testing input data, which varied NMAE of the input data error from 1.81% to 8.19%. In the Figure 7 the blue line is input NMAE error and the red line is corresponding output NMAE error. The output error starts with a non-zero value because of initial error of ANFIS5trimf model for the testing sample. The NMAE error of the output data of the testing sample varied from 4.19% to 5.78%, on the basis of which we can conclude that the calculations showed a sufficiently low level of variation in the output values relative to the error of the input data.

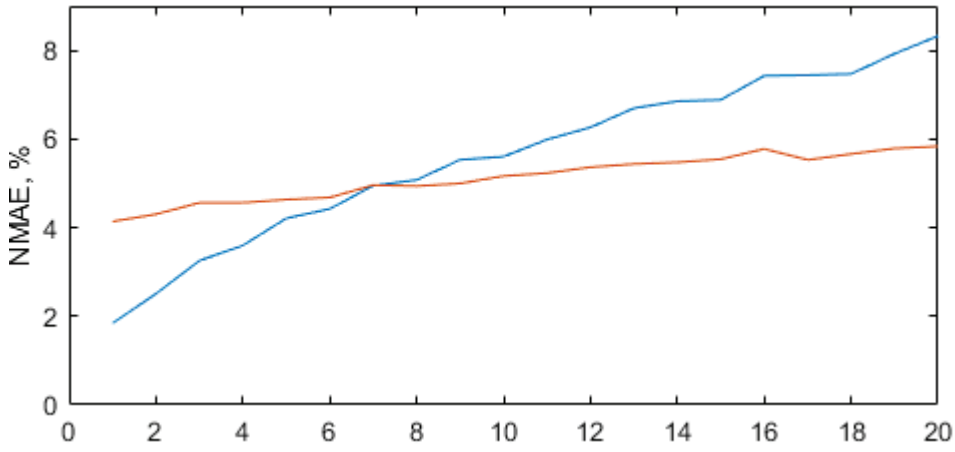

FIGURE 7. *The input data NMAE error (blue line) and corresponding output NMAE error (red line)*

Conclusions

The study demonstrates an algorithm according to which it is proposed to study the structure and sensitivity of ANFIS-based models for the problem of approximating the dependence of SPP generation power on solar irradiance. In this study, the best type of membership function was trimf, the number and shape of functions had little effect on the result – within 0.23% of NMAE.

Regarding the sensitivity of the model to the input error, it can be concluded that for 5 input trimf membership functions, increasing the input error to 8.19% NMAE leads to an increase in the output error in the testing sample to 5.78%, NMAE. The rather low sensitivity of the model to the input data error allows us to conclude that it can be used for forecast meteorological data with a pre-known fixed forecast error.

Conflicts of Interest: The author declares no conflict of interest.

References

[1] Akhter M.N., *ANFIS: Review on forecasting of photovoltaic power generation based on machine learning and metaheuristic techniques*. Akhter M.N., Mekhilef S., Mokhlis H., Shah N.M., IET Renewable Power Generation 2019, Vol. 13, Iss. 7, pp. 1009-1023.

[2] Installed capacity of the IPS of Ukraine values. Available at: https://ua.energy/vstanovlena-potuzhnist-energosystemy-ukrayiny (Accessed: 30 April 2021).

[3] Jang J.-S.R., *ANFIS: Adaptive-Network-Based Fuzzy Inference System*. Jang J.-S.R., IEEE Transactions on Systems, Man, and Cybernetics 2018, Vol. 23, No. 3, pp. 665-685.

[4] Photovoltaic (PV) Solar Panel Energy Generation data. Available at: https://data.london.gov.uk/dataset/photovoltaic--pv--solar-panel-energy-generation-data (Accessed: 30 April 2021).

[5] Semero Y.K., *PV Power Forecasting Using an Integrated GA-PSO-ANFIS Approach and Gaussian Process Regression Based Feature Selection Strategy*. Semero Y.K., Zhang J., Zheng D., CSEE Journal of Power and Energy Systems 2018, Vol. 4, No. 2, pp. 210-218.

[6] Wu Y.-K., *A Novel Hybrid Model for Short-Term Forecasting in PV Power Generation*. Wu Y.-K., Chen C.-R., Rahman H.A. International Journal of Photoenergy 2014, 9 p.

[7] MATLAB documentation. Available at: https://www.mathworks.com/help (Accessed: 30 April 2021).

Oleksii LYMARENKO

Poltava National Technical Yuriy Kondratyuk University

DOI: 10.53412/jntes-2021-1.6

EFFECT OF GEOTHERMAL ENERGY PRODUCTION ON ECOLOGICAL ENVIRONMENT IN UKRAINE

Abstract: *General potential of geothermal resources of Ukraine and the possibilities of their use as an alternative fuel are considered in the article. The most promising regions of Ukraine for the development of geothermal energy were determined and the characteristics of the heat-transfer agent were described. Value engineering analysis of modern technologies of extraction of heat was carried out, taking into account a feasibility study. Possibilities of using depleted oil and gas fields were studied, as well as the simultaneous use of wells for the extraction of hot water and hydrocarbons. The factors that affect the extent of the use of geothermal energy were examined. The important aspects of the use of geothermal energy sources, such as renewability, getting a heat-transfer agent of much lower temperature than from firing, combination of the energy use and minimal detrimental impact on the environment were listed. There were also described the disadvantages of use of geothermal resources, such as the need to use at the place of production, the high cost of construction of wells with increased depth, swamping the area, release into the atmosphere of dissolved sulfur compounds, mercury, arsenic and boron. Methods to reduce harmful emissions into the environment of geothermal power plants were proposed.*

Keywords*: energy, energy conservation, alternative energy sources, geothermal power plants, hydrothermal energy.*

Introduction

The rapid development of civilization in the last decade, which is inseparably linked with the constant increase of resource consumption, raises once again the question of optimal consumption of fuel resources.

In Ukraine there are 20 times more of explored geothermal resources [1] than of all together calorific natural resources (oil, gas, condensate, coal, peat, wood, vegetable and biological masses).

Despite the seeming simplicity and availability of geothermal energy use with the help of turbines and turbogenerators connected to them, the technical and environmental implementation of this method of generating electricity is a complex scientific and technical challenge. Technologically and economically developed countries such as the USA, the Philippines, Mexico, Italy and Japan for the last 20 years have increased the costs of creating new geothermal technologies up to 2 billion US dollars.

Object, purpose and tasks of the research

The object of the research is geothermal well and operation of geothermal heat station for heat and cooling of facilities of housing and communal services.

The purpose of the research is to determine the factors that affect the environmental safety of use of geothermal resources in Ukraine.

Given the purpose of the research, the authors have set the following tasks:

- to determine the geothermal potential of Ukraine;
- to examine the economic performances of hydro-thermal resources;
- to indicate promising areas of their development;
- to consider the scope of use of geothermal resources;
- to identify the main advantages and disadvantages of use of geothermal waters.

Identification of the main environmental factors while using geothermal resources

Ukraine has a considerable potential of geothermal energy. This is due to the geothermal peculiarities of the relief and to the peculiarities of geothermal resources of the country. The geothermal resources include, first of all, thermal water and the warmth of the heated dry rocks. Promising for use in commercial volumes are the resources of thermal water, which is extracted along with oil and gas on the respective fields.

Scientific and practical research work in Ukraine is focused now only on geothermal resources, which are represented by hot waters. According to various estimates, there are about 8.4 million tons of oil equivalent per year of economically viable energy sources of hot water in Ukraine. There are enough geothermal areas In Ukraine with potential for high temperature (120-180°C), which allows the use of geothermal fields with high temperature for electricity production.

In Ukraine, there were sunk more than 12 thousand wells to determine the thermal field, most of which have been studied in detail by leading scientists and researchers of Ukraine. On the basis of these data the atlas of geothermal energy at different depths has been compiled.

The thermal energy of the Earth, as described in [2], is an energy resource. Solar energy resources of Ukraine on the projected depth characterize the thermal-physic parameters of the Earth, namely, the temperature and the density of the heat flow. According to the conducted researches, it is possible to separate two areas of distribution of geothermal resources (35-50 mW/m^2) and abnormal (60-130 mW/m^2) on the territory of Ukraine.

The most promising regions of Ukraine for the development of geothermal energy are Luhansk, Kharkiv, Donetsk and eastern part of Dnipropetrovsk regions (about 12 million people) with the depths of the wells up to 3000 m; western part of Dnipropetrovsk, Poltava, Chernihiv and Sumy regions (about 5.3 million people) with the depths of the wells up to 3500 m. On the west of the country: Lviv, Ivano-Frankivsk, Chernivtsi and Zakarpattia regions (about 6.2 million people) with the depths of the wells up to 3000 m. On the south there are Odessa, Mykolaiv, Kherson and the whole Crimean peninsula (about 7.5 million people), where wells will have the depth of 3000 m [3].

Every fourth well in Poltava and Ivano-Frankivsk regions can be used to receive energy. Large-scale use of this type of geothermal resources doesn't require any preliminary preparatory works, separate geological exploration, drilling of industrial wells or substantial investment.

Cost-effective for use in future are the resources of low-grade heat of natural and anthropogenic origin, which can be utilized by heat pumps, and are estimated at 22.7 million e.f. at the level of the year 2030.

Among all types of geothermal energy, the best economic indexes have hydro-geothermal resources – thermal waters, steam-water mixtures and natural steam [4].

Experts of the state agency for efficiency and energy saving of Ukraine note that if the entire world switched to the use of geothermal energy, to decrease the temperature of the earth's interior by only half a degree would take 41 billion years.

Hydro-geothermal resources, which are used to produce electricity, account 4% of the total explored reserves, that is why their use in the future should be viewed along with heating of local facilities.

Large-scale use of geothermal energy is determined by several factors: the need to finance the construction of wells, the price of which increases with increase of the depth. Thermal waters can be used in two ways: fountains (hot water is discharged into a local pond) and circulations (hot water is re-injected into the well).

The first way is simpler and requires less financial costs, but it is environmentally unsafe, the second way is more expensive, but its use ensures the preservation of the environment [5].

Today, Ukraine attaches a lot of importance to the problem of energy conservation and efficiency, to solve it is on the first place for its strategic development. This issue has become particularly sensitive after the gas crisis between Russia and Ukraine on "blue fuel" supplies. As is known, Ukraine belongs to the energy deficient countries. Annual technically achievable energy potential of geothermal energy in Ukraine is the equivalent of 12 million tons e.f., its use would allow to save about 10 billion m^3 of natural gas [6].

The development and use of alternative energy is important not only because of the exhaustion of fossil fuels, but also because of the devastating global impact on the environment. An important aspect of the use of alternative energy sources is their environmental friendliness.

Developing countries will increase the share of energy consumption three times, and the volume of carbon dioxide emissions will annually increase by 2.1%. This scenario represents a real threat to global man-made climate changes, that is why the importance of renewable and environmentally friendly alternative sources of energy will certainly increase [7].

International congress on geothermal energy in the city of Florence found it in comparison with other alternative energy sources as the most advantageous, environmentally clean, safe and cheap.

Geothermal energy source influences on the environment in different ways. The additional amount of dissolved in geothermal waters compounds of sulfur, boron, arsenic, ammonia and mercury is discharged into the atmosphere; steam appears; humidity increases; emissions of steam are accompanied by acoustic effects; failures of the earth's surface; the geothermal brine enters the soil.

The advantage of use of geothermal power plants is their environmental friendliness. Waste waters are pumped back into the well, it would ensure the environmental safety of the region and the stability of the engineering procedure. Geothermal power plants produce significantly fewer harmful emissions into the atmosphere – a geothermal station produces CO_2 emissions on 1 mW/h of the produced energy at a rate of 0.45 kg, while the thermal power plant fueled by natural gas – 464 kg, on fuel oil – 720 kg, on the coal – 819 kg [8].

To install a geothermal power plant there is a need in a relatively smaller plot of land than for the construction of thermal power plants. They can be placed even in a resort area.

Geothermal power plants have a negative impact on the environment during the development of the field, steam pipeline installation. This impact is usually limited to the area of the field.

Hot water or steam is produced by means of wells, which are drilled to a depth of 300 m to 2700 m. Under the influence of geostatic pressure the heat carrier rises to the surface, where it is used in turbines [9].

The negative effects of extraction of geothermal heat carriers are failures of soil and earthquakes. Failures of soil can be observed throughout the field, due to the lowering of the lower layers of soil, which are pressured by the upper layers. The production of geothermal sources may be further reduced.

Increased seismic activity may be a sign of existence of the thermal fields, it is often used in exploration.

However, there is no reason to believe that the production of geothermal resources can lead to an increase in seismic activity in the region. Since the number of earthquakes in the area of development of geothermal fields caused by volcanic action is much less than the intensity of the earthquakes that occur as a result of crustal movements along the faults.

The technological process of the production of electrical energy on geothermal heating station does not require burning fossil fuels. Therefore the amount of harmful gases emission to the atmosphere is much less than on the thermal power plants and its chemical composition differs from the emissions of stations on a gaseous fuel. Produced by geothermal stations steam is essentially water vapour. 80% of gas impurity is carbon dioxide and a small proportion of methane, hydrogen, nitrogen, ammonia and hydrogen sulfide. The most dangerous and harmful is hydrogen sulfide (0.0225%). The composition of geothermal waters includes the following dissolved gases: SO_2, N_2, NH_3, H_2S, CH_4, H_2 [10].

Cooling water consumption on geothermal plants (per 1 kWh of electricity produced) is 4-5 times higher than on the heat power plant. It is because of a lower coefficient of efficiency. Cooling of used heat carrier in local reservoirs can lead to their thermal pollution, the increase of concentration of salt, sodium chloride, ammonia, silica, and of such elements as boron, arsenic, mercury, rubidium, cesium, potassium fluoride, sodium bromine and iodine albeit in small quantities. With increasing depth of wells the concentration of these harmful substances can grow [11].

During exploitation of geothermal heat plants, the contamination of surface and groundwater aquifers is possible due to the release of solutions with a high concentration during drilling operations. Discharge of the used heat carrier can lead to waterlogging of the areas in high humidity climate, and in the areas with dry climate to increase of the salt concentration. At the break of the pipeline a large amount of brine can get on the surface of the soil.

Efficiency of geothermal power plants is 2-3 times lower than that of nuclear power plants and thermal power plants, and they emit 2-3 times more of the heat. To reduce the harmful effects on the environment the use of a circular circulation of the heat carrier on geothermal plants should be encouraged under the scheme system "well – waste-heat recovery units – well – layer". In turn, this will enable us to reduce the flow of heat carrier to the surface of the soil, in the groundwater aquifers and lakes, will enable to keep reservoir pressure, to exclude ground failures and to reduce seismic activity.

Adverse environmental impacts of geothermal energetics:

- alienation of land;
- changes in the level of groundwater, soil failures and waterlogging;
- gas emissions (methane, hydrogen, nitrogen, ammonia and hydrogen sulphide);
- release of heat into the atmosphere or into surface waters, which create a local increase in humidity and is accompanied by an acoustic impact;
- reset of the poisoned water and condensate, contaminated with small quantities of ammonia, mercury and silica;
- pollution of groundwater and aquifers, soil salinity;
- emissions of large amounts of brine at break of pipelines;
- emissions of radioactive elements together with the steam;
- changes in temperature fields of layers.

Conclusions

As the result of the conducted researches there has been determined:

1. Geothermal potential of Ukraine, the main promising regions for the use of geothermal energy.
2. In order to reduce costs for the construction of geothermal wells it is proposed to use depleted oil and gas wells.
3. The causes that complicate the use of thermal water in the heating energy sector have been described.
4. The main spheres of the large-scale use of thermal waters for heating, hot water supplies, cooling and extraction of valuable chemical components have been determined.

5. The advantages and disadvantages of the use of geothermal energy and the typical diverse impact of geothermal sources on the environment have been analyzed.
6. The most harmful toxic gases, contained in dissolved form in geothermal waters, such as hydrogen sulfide, sulfur oxide, nitrogen, ammonia and methane have been revealed.
7. A comparative analysis of the coefficient of efficiency of geothermal station with nuclear power station and warm power station has been conducted. There has been discovered that the efficiency of a geothermal station is in 2-3 times lower, but at the same time there are 2-3 times less of heat pollutant emissions.

Conflicts of Interest: The author declares no conflict of interest.

References

[1] Beloselskii B.S. (2005), *Technology of fuel and energy oils*. Moscow: publishing office. University, 346.

[2] Klavdienko B.P. (2006), *Alternative energy in the EU*. Moscow, Science, 42-43.

[3] Sibikin U.D. (2008), *Renewable energy sources*. Moscow, 228.

[4] Shydlouski A.K. (2007), *Energy efficiency and renewable energy*. Ukrainian encyclopedic knowledge. Kyiv, 559.

[5] Belaev L.S. (2004), *Energy XXI Century: Terms of development, technology forecasts*. Novosibirsk, Science, 356.

[6] Denis O.B. (2008), *House "zero" energy ... because Earth and the sun does not bill*. Lviv, 336.

[7] Dakovski V.M. (2007), *On energy for consumers and skeptics*. Ekoinform, 212.

[8] Zabarnii G.N. (1999), *Technical and economic feasibility study of industrial development for the purpose of heating the thermal waters*. Transcarpathian region. Kyiv, 247.

[9] Kudra S.O. (2007), *Prospects for the replacement of traditional energy resources by energy generated at the Alternative Energy. Energy saving*. Ukrainian scientific and technical journal, 14-22.

[10] Luescher M. (2004), *Temperature distribution in karst systems: the role of air and water fluxes*. Terra Nova, 350.

[11] Klimenko P.P. (2000), *Tehnoekologiya*. Odessa, 542.